Yukawa Institute of Theoretical Physics. HHIQCD-Workshop, Kyoto, Japan.

Baryonic Strings in Pure Yang-Mills theory

Presenter: Ahmed Bakry.

Collaborators:

Xurong Chen, Pengming Zhang.

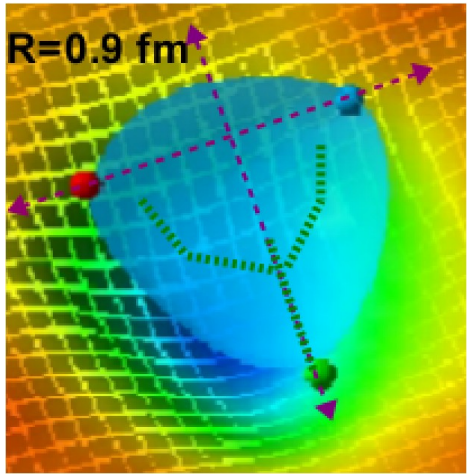

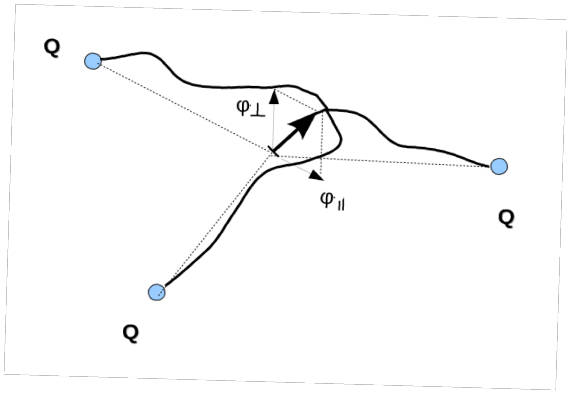

Institute of Modern Physics, Chinese Academy of sciences

A. S. Bakry, X. Chen, and P.-M. Zhang (2014), hep-lat/1412.3568

Talk summary

- Motivation.
- Baryonic String Model.
- Measurements and Noise Reduction.
- Results.

Motivation

- The string picture is successful in the IR region of QCD.

- The string picture's implies the Luscher subleading correction to the QQ potential .

$$V(r) = \sigma r + \mu - \frac{\pi}{24r}(d-2)(1+b/r)$$

- Effective bosonic strings logarithmic growth property.

$$W^2 = \frac{(D-2)}{2\pi\sigma} log(R/R_0)$$

- Verified on the lattice at large distances in many gauge models.

- The stringlike behaviour of flux tubes in multi-quark systems is less visited on the lattice due to the noisy signal.

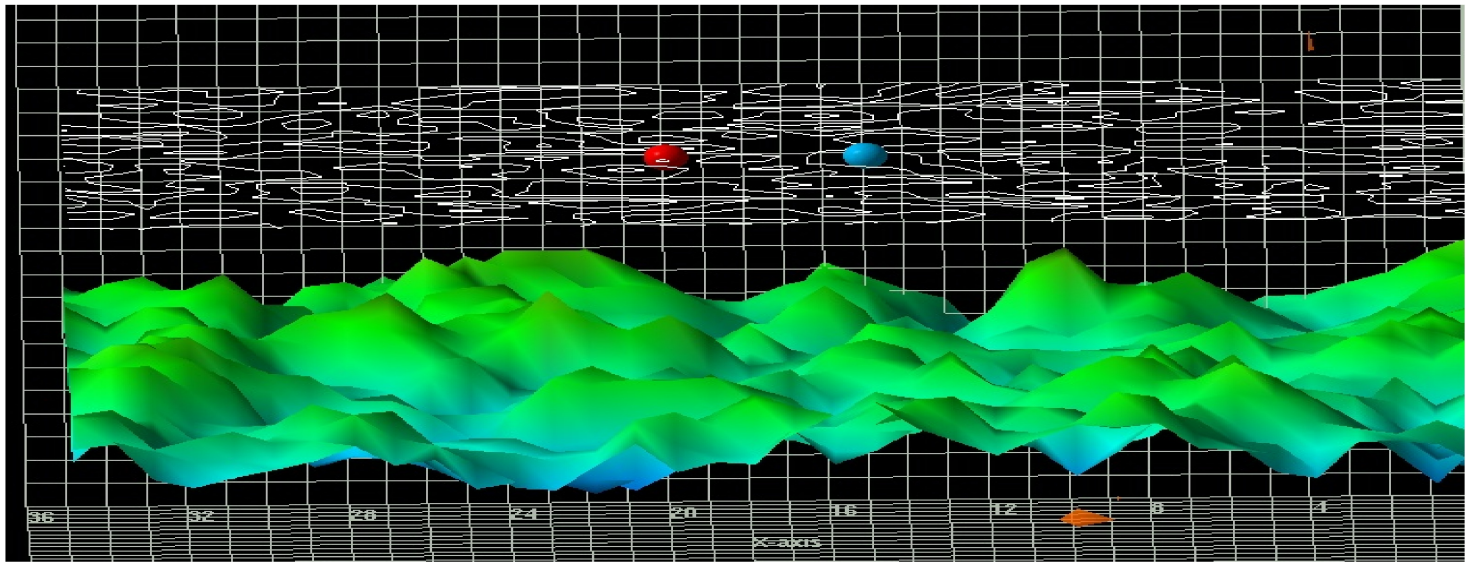

- This has presented hitherto a challenge to directly scrutinize the baryonic strings on the lattice unambiguously.

Lattice QCD findings regarding the 3-quark potential are settled about a confining potential that admits two possible models depending on the inter-quark separation distances.

$$V_{qqq}(\vec{r}_1, \vec{r}_2, \vec{r}_3) \approx \frac{1}{2} \sum_{i<j} V_{q\bar{q}}(r_{ij})$$

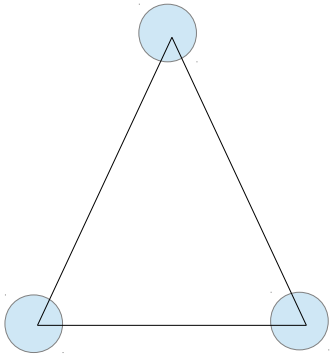

The so-called Delta parametrization for small quark separation distances of R<0.7 fm and the Y-ansatz for R >0.7 fm.

C. Alexandrou, P. de Forcrand, and O. Jahn, Nucl. Phys. Proc. Suppl. 119, 667 (2003), hep-lat/0209062.

$$V_{3Q} = -A_{3Q} \sum_{i<j} \frac{1}{|\mathbf{r}_i - \mathbf{r}_j|} + \sigma_{3Q} L_{\min} + C_{3Q},$$

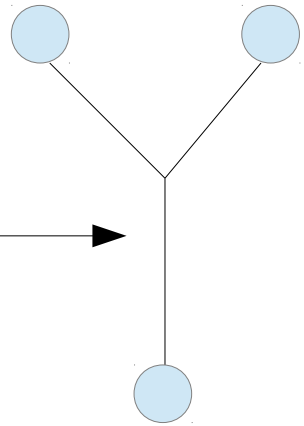

Genuine three-body force

N. Brambilla, J. Ghiglieri, and A. Vairo, Phys.Rev. D81,054031 (2010), 0911.3541. (Perturbative calculations)

- Unexpected filled Δ-shaped flux arrangement surprisingly persists to large inter-quark separations.

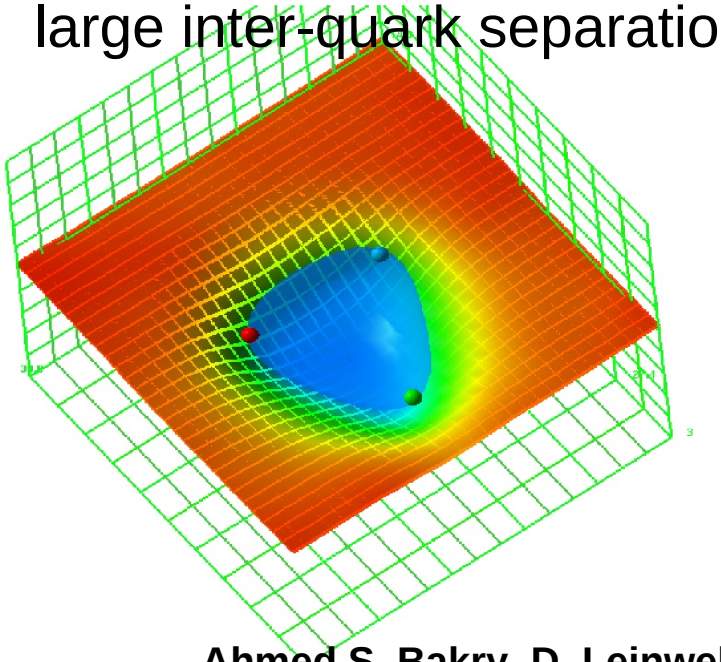

Ahmed S. Bakry, D Leinweber, Tony Williams, arXiv:1107.0150 [hep-lat]

- A baryonic string model indicates Lüscher-like terms that has been addressed in 3 Potts model.

O Jahn and Ph. Deforcrand, hep-lat/0209062, Ph. De Forcrand and O. Jahn, N phys A 755(2005)

Baryonic String Picture

Model assumptions

The elementary constituents of hadronic matter (quarks) are confined together due to formation of very thin flux tubes.

In the Y-baryonic string model. The quarks are connected by three strings that meet at a junction.

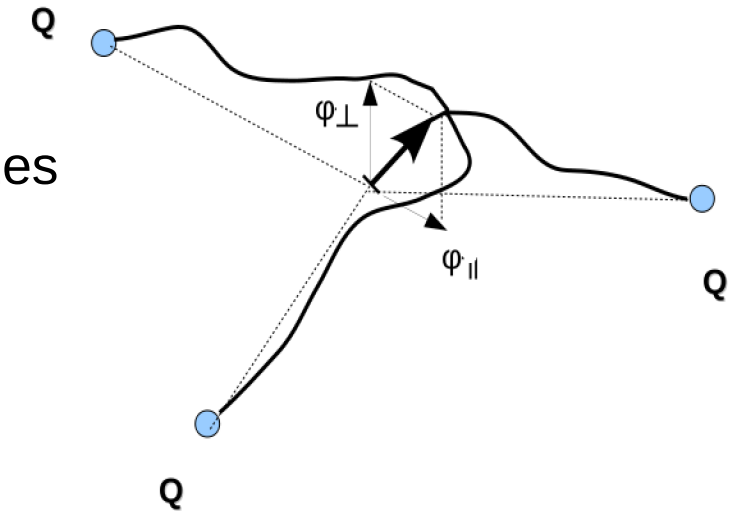

The classical configuration is the one that minimizes the area of the string world sheets.

The position of the junction is determined by the requirement of minimal total string length.

- The most natural choice for the string action S is the Nambu–Goto action which is proportional to the surface area of the world sheet.

$$S[X] = \sigma \int d\zeta_1 \int d\zeta_2 \sqrt{g},$$

$g_{\alpha\beta}$ is the two dimensional induced metric on the blade world sheet embedded in the background R4.

$$g_{\alpha\beta} = \frac{\partial X}{\partial \zeta_\alpha} \cdot \frac{\partial X}{\partial \zeta_\beta}, \quad (\alpha, \beta = 1, 2),$$

$$g = \det(g_{\alpha\beta}).$$

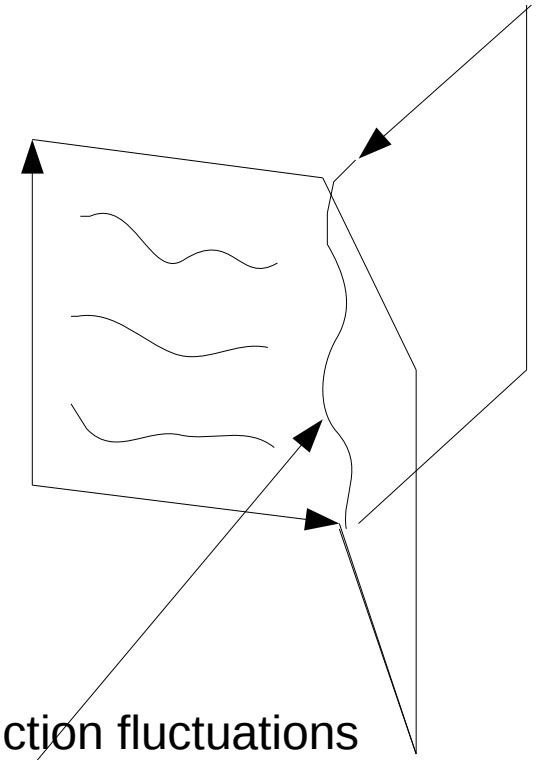

The string partition function is a Gaussian integral over the junction fluctuations

$$Z = e^{-(\sigma L_Y + m) L_T} \int D\varphi \ \exp\left(-\frac{m}{2} \int dt \, |\dot{\varphi}|^2\right) \prod_{i=1}^{3} Z_i(\varphi),$$

$$Z_i(\varphi) = \int_\varphi D\xi_i \ \exp\left(-\frac{\sigma}{2} \int |\partial \xi_i|^2\right)$$

The partition function for the fluctuations of a given blade that is bounded by the junction worldline φ(t)

Baryonic string models

Evaluating the determinant of the Laplacian based on conformally mapping generalized domains of the blade (corresponding to each string) to rectangles.

O Jahn and Ph. Deforcrand, hep-lat/0209062, Ph. De Forcrand and O. Jahn, N phys A 755(2005)

$$Z_i(\varphi) = e^{-\frac{\sigma}{2}\int |\partial \xi_{\min,i}|^2} \left|\det(-\triangle_{\Gamma_i})\right|^{-(D-2)/2}$$

$$f_a(z) = z + \frac{1}{\sqrt{T}} \sum_{w\neq 0} \frac{e_a \cdot \varphi_w}{\sinh(wL_a)} e^{wz} + O(\varphi_w^2).$$

.

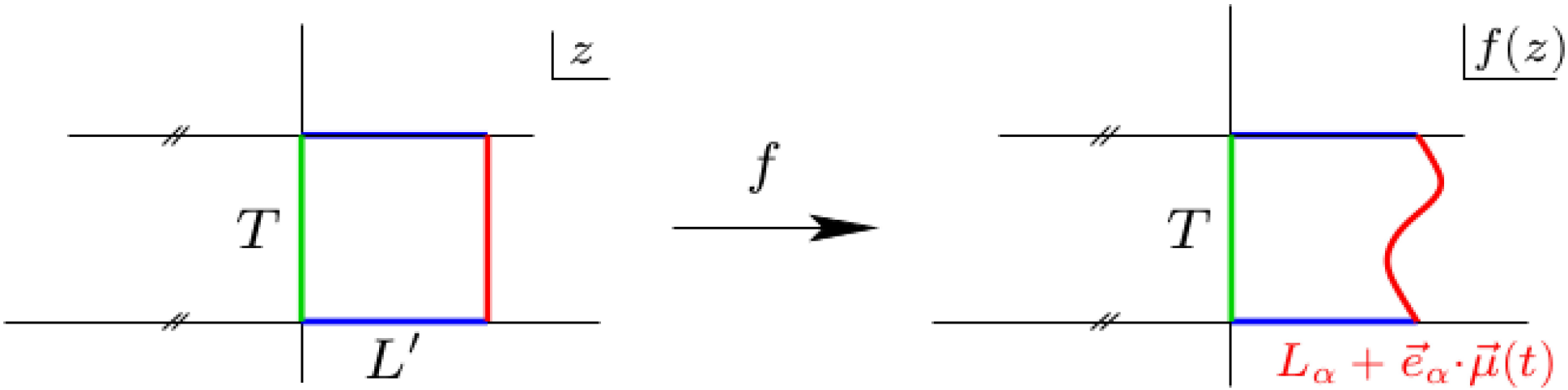

$$\triangle_{\Gamma_a} = e^{2\rho_a(z)} \triangle_{L'_a \times T}\,, \quad \rho_a(z) = -\frac{1}{2} \ln \left|\partial_z f_a\right|^2 .$$

$$V_{qqq}(L_1, L_2, L_3) = \sigma \sum_i L_i + V_{\parallel} + V_{\perp} + O(L_i^{-2}) \,,$$

with

$$V_{\parallel} = -\frac{\pi}{24} \sum_i \frac{1}{L_i} + \int_0^{\infty} \frac{dw}{2\pi} \ln \left[\frac{1}{3} \sum_{i<j} \coth(wL_i) \coth(wL_j) \right] \,,$$

$$V_{\perp} = -\frac{\pi}{24} \sum_i \frac{1}{L_i} + \int_0^{\infty} \frac{dw}{2\pi} \ln \left[\frac{1}{3} \sum_i \coth(wL_i) \right] \,.$$

The first test of the baryonic string model predictions with LGT at zero temperature has been reported by Deforcrand and Jahn considering 3 Potts model for a three quark potential.

The numerical measurements of the 3-state Potts gauge model are consistent with the predicted Lüscher-like corrections and the formation of a Y-system of three flux tubes.

Pfufer, Bali, and Panero extended the calculations of the above model to the thickness of the fluctuating baryonic junction.

$$\langle \varphi^2 \rangle = \frac{\int D\varphi\, \varphi^2 e^{-S}}{\int D\varphi\, e^{-S}} \,.$$

$$\langle \varphi_\perp^2 \rangle = \frac{2}{L_T} \sum_{w>0} \frac{1}{mw^2 + \sigma w \sum_i \coth(wL_i)}$$

with $w = 2\pi n / L_T$.

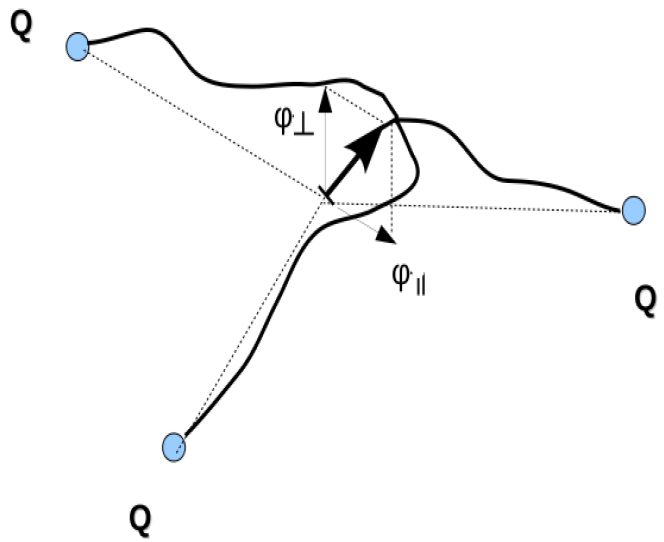

They have shown a logarithmic growth of the junction width for equilateral triangle configurations.

M. Pfeuffer, G. S. Bali, and M. Panero, PRD 79, 025022 (2009).

Smoothing the conformal mapping.

At finite temperature, we need to smooth over the first order fluctuations of the junction to account for higher order terms which can become relevant at finite temperature.

$$f_a(z) = z + \frac{1}{\sqrt{T}} \sum_{w \neq 0} \frac{e_a \cdot \varphi_w \psi(wL_a)}{\sinh(wL_a)} e^{wz}$$

$$\triangle_{\Gamma_a} = e^{2\rho_a(z)} \triangle_{L'_a \times T}\,, \quad \rho_a(z) = -\frac{1}{2} \ln |\partial_z f_a|^2\,.$$

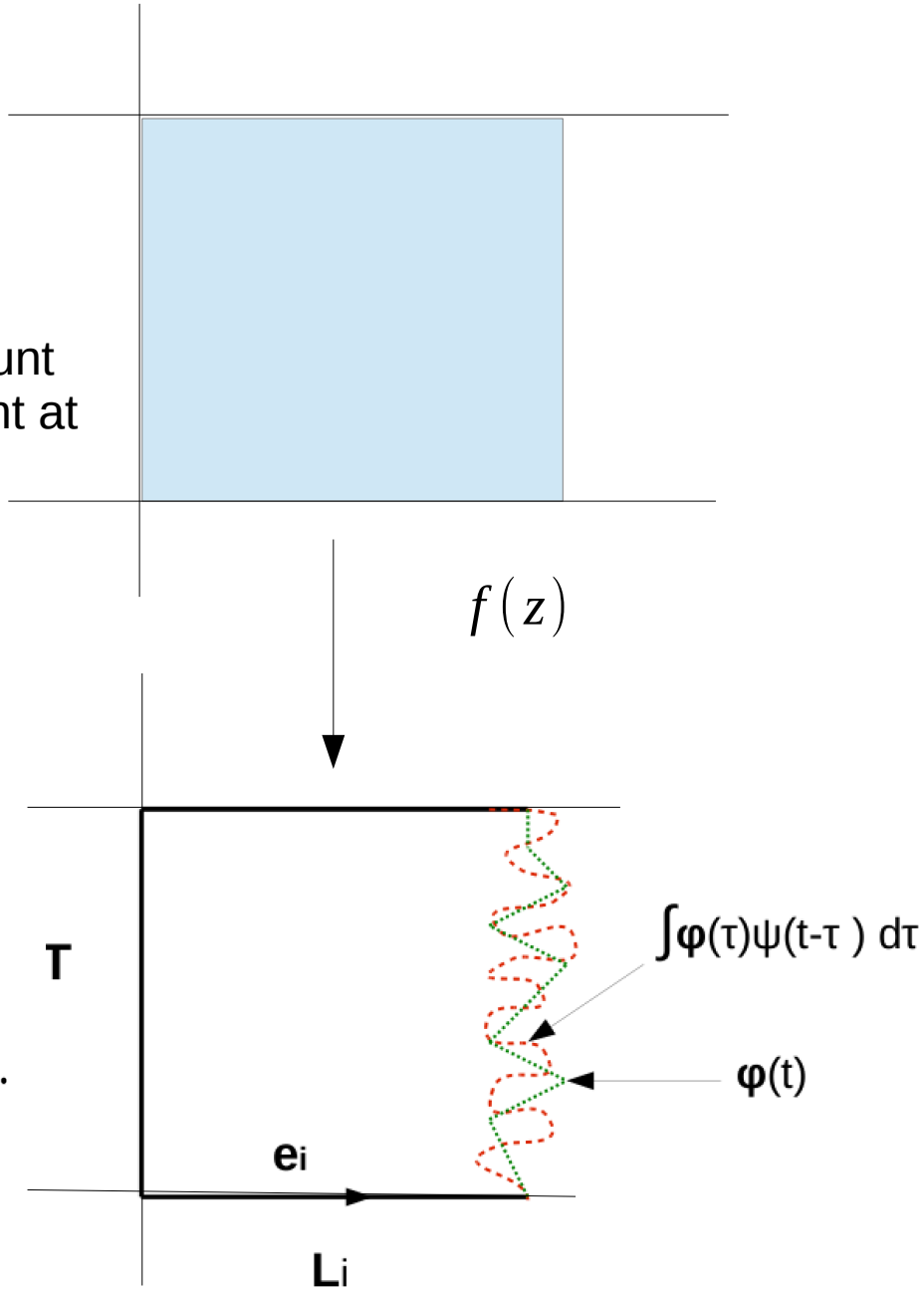

Smoothing the leading-order terms

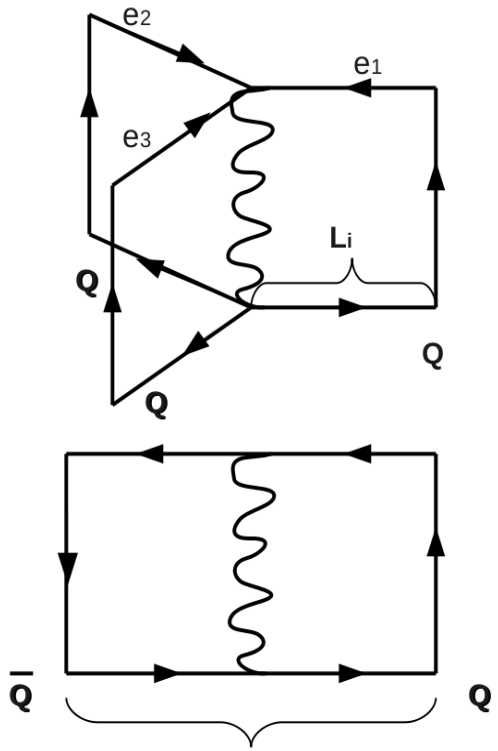

Smoothing scalar can be found from the mesonic limit.

A. Allais and M. Caselle, J. High Energy Phys. 01 (2009) 073, arXiv:0812.0284 [hep-lat].

$$\psi(\omega, L_i) = \frac{-k\omega}{2\sigma \coth(\omega L_i)} - \frac{(\omega L_T - \pi)}{2\omega L_T \coth(\omega L_i)} \left(\frac{2L_i \chi(\tau_i) + 1}{2L_i \chi(\tau_i) - 1} \right)^{\omega L_T/\pi - 1}$$

where $\chi(\tau) = \dfrac{\theta_2(0;\tau)}{\theta_1'(0;\tau)}$, $\theta_{1,2}$ are Jacobi theta functions, and $\tau = \frac{L_T}{R}$ being the modular parameter of the cylinder, and $L_T = 1/T$ is the temporal extent governing the inverse temperature.

The junction fluctuations decomposed into perpendicular

$$\langle \phi_z^2 \rangle = \frac{2}{L_T} \sum_{\omega>0} \frac{1}{k\omega^2 + \sigma\omega \sum_i \coth(\omega L_i)\psi(\omega, L_i)}.$$

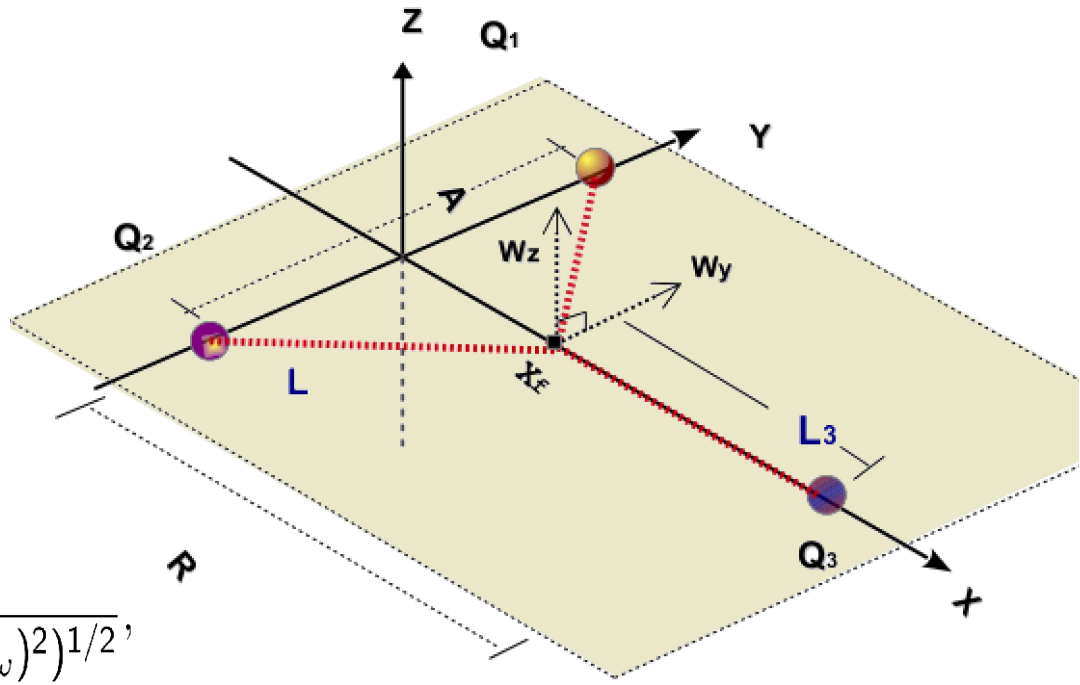

and parallel fluctuations

$$\langle \phi_x^2 \rangle = \frac{2}{L_T} \sum_{\omega>0} \frac{1}{Q_{x,\omega} + Q_{y,\omega} - (Q_{xy,\omega}^2 + (Q_{x,\omega} - Q_{y,\omega})^2)^{1/2}},$$

$$\langle \phi_y^2 \rangle = \frac{2}{L_T} \sum_{\omega>0} \frac{1}{Q_{x,\omega} + Q_{y,\omega} + (Q_{xy,\omega}^2 + (Q_{x,\omega} - Q_{y,\omega})^2)^{1/2}}.$$

to the 3 quark plane would read as a sum over Fourier modes as above.

$$Q_x = \left(k\omega^2 + \sigma\omega \sum_i \coth(\omega L_i)\psi(\omega, L_i) \right) +$$

$$\left(\frac{\sigma}{2}\omega + \frac{\omega^3}{12\pi} \right) \left[\sum_i \eta_{i,x}^2 \coth(\omega L_i)\psi(\omega, L_i) \right],$$

The string fluctuations are smoothed and decoupled to make it more convenient to compare with lattice data at finite temperature.

The string fluctuations are smoothed and decoupled to make it more convenient to compare with lattice data at finite temperature.

We summarize the motivation to discuss an effective Y-string model versus the lattice data at high temperature in the following main points:

The linear growth property of the confining flux-tube at high temperature has been verified on the lattice.

That is, no substantial changes in the nature of the confining thin tubes between a quark-antiquark pair on large distance scales.

The Y-model seems consistent with lattice data corresponding to the confining potential at T = 0.

Lattice Measurements: Field correlators

The form of the correlation function for the action density,

$$C(\vec{y},\vec{r}_1,\vec{r}_2,\vec{r}_3) = \frac{\langle \mathcal{P}_{3Q}(\vec{r}_1,\vec{r}_2,\vec{r}_3)\, S(y,t)\rangle}{\langle \mathcal{P}_{3Q}(\vec{r}_1,\vec{r}_2,\vec{r}_3)\rangle \,\langle S(y,t)\rangle}$$

where $\mathcal{P}_{3Q}(\vec{r}_1,\vec{r}_2,\vec{r}_3) = P(\vec{r}_1)\,P(\vec{r}_2)\,P(\vec{r}_3)$.

C is a scalar field in three dim.

C = 1

C < 1

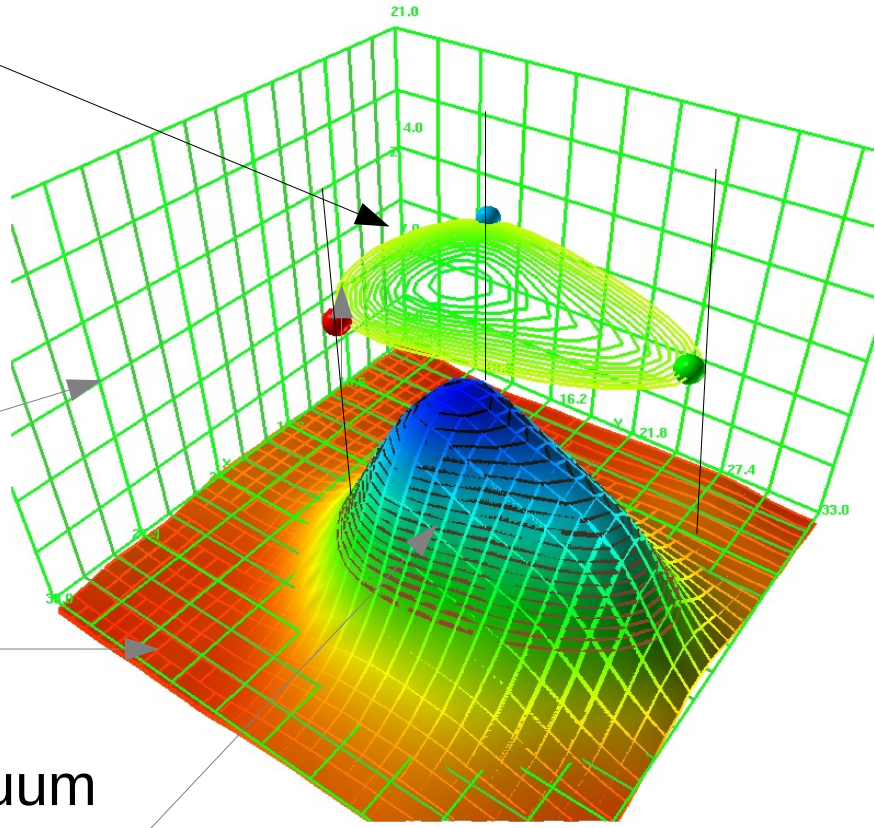

$\vec{r}_i$

- C < 1, signaling the expulsion of the vacuum fluctuation from the interior of the Baryonic system.

Simulation set-up

The gauge configurations were generated using the standard Wilson gauge action.

The two lattices employed are of spatial size corresponding to N_s=36, and temporal extents corresponding to N_t=,10, 8.
beta=6.0, lattice spacing a=0.1 fm.

Bins of 20 measurements separated by 70 sweeps of updates.
Each bin of measurements is taken following a 2000 of updating sweeps.

500 bins corresponding to 10,000 measurement at each temperature.

Smearing Radius

A=0.6 fm

To ensure minimal effect of 4 -D smearing on the 3Q potential the smearing Sphere around each quark should be Non-overlapping.

A=0.8 fm

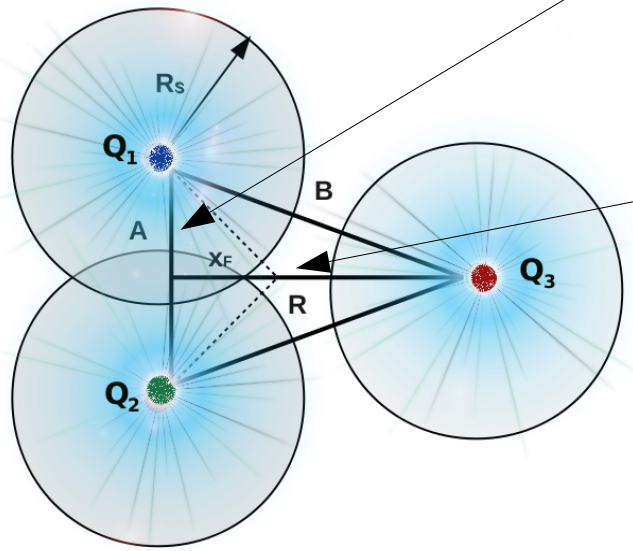

A=1.0 fm

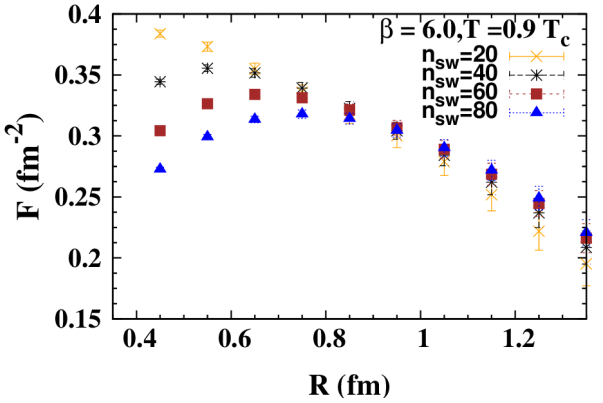

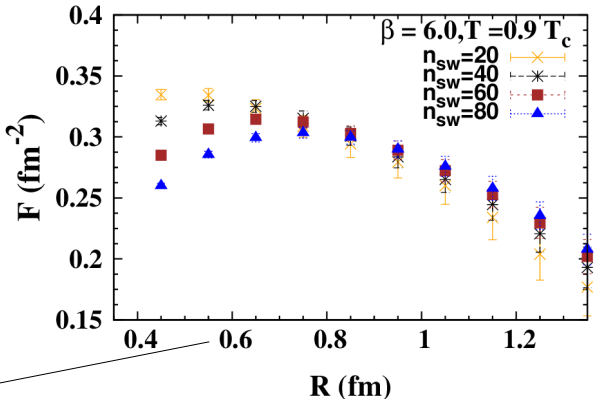

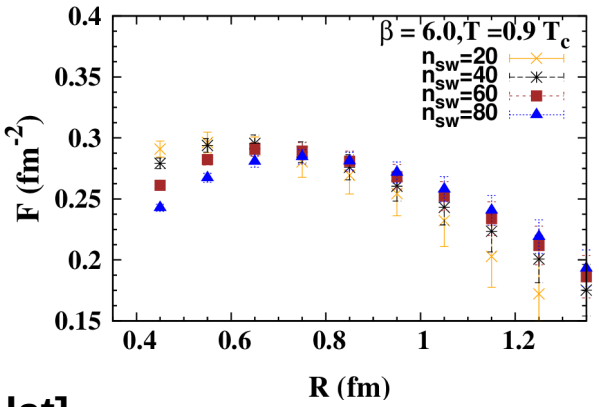

A. Bakry et al., Phys. Rev. D 82 (2010) 094503, arXiv:1004.0782 [hep-lat].

In particular, the evaluation of Polyakov loop correlators on cooled lattices, where the temporal links are included in the link-blocking, leads to a systematic ambiguity in regard to the transfer matrix interpretation which allows one to identify the expectation values of the Polyakov loop correlators with exp(−V (R, T)/T).

Although one can approximately preserve this interpretation only for the measurements of correlators carried out on distance scales larger than the diameter of the Brownian motion of a diffused link, this restricts the applicability of the 4D smearing or “cooling” technique to high temperatures or small loops size.

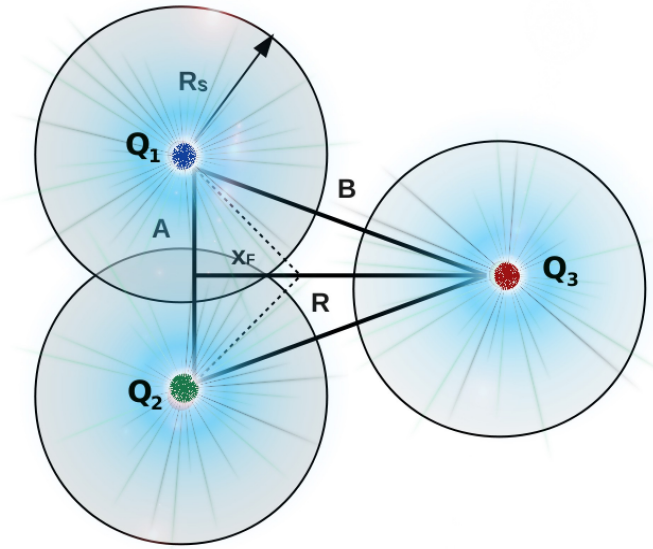

Noise reduction: Noise reduction by combining smearing with multi-level integration methods.

The simultaneous application of both link-blocking and path-integral factorization techniques.

A measurement of the field-strength operator can be performed together with the trace of the products in the lowest level estimates.

$$\langle P(x)P^{\dagger}(x+R)S(\vec{r})\rangle = \langle[[\mathbb{T}(t_0)][\mathbb{T}(t_0+a)]]..[[\mathbb{T}(T_{N_t}-a)][\mathbb{T}(T_{N_t})]]_{\alpha\alpha\gamma\gamma}$$

The key objects in this factorizing are the tensor prod

$$\mathbb{T}(t_0)_{\alpha\beta\gamma\delta} = U(x,t_0)_{\alpha\beta}U^{\dagger}(x+R,t_0)_{\gamma\delta},$$

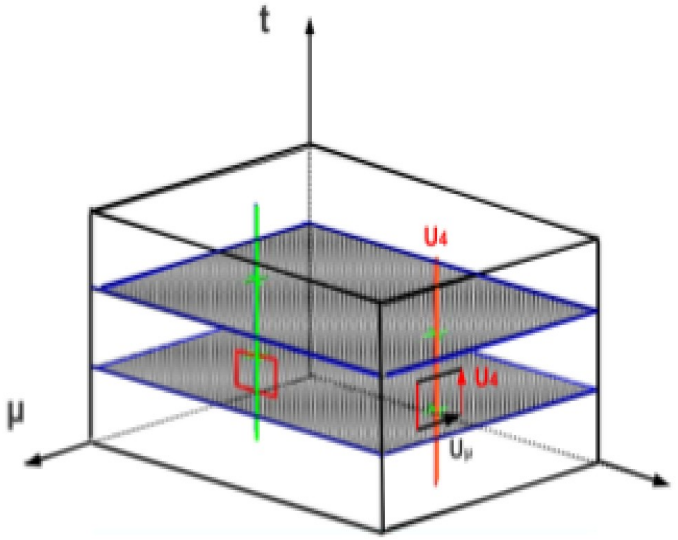

- Based on the observation that Monte-Carlo updating of the three-dimensional smeared lattices preserves the key features of the long distance physics.

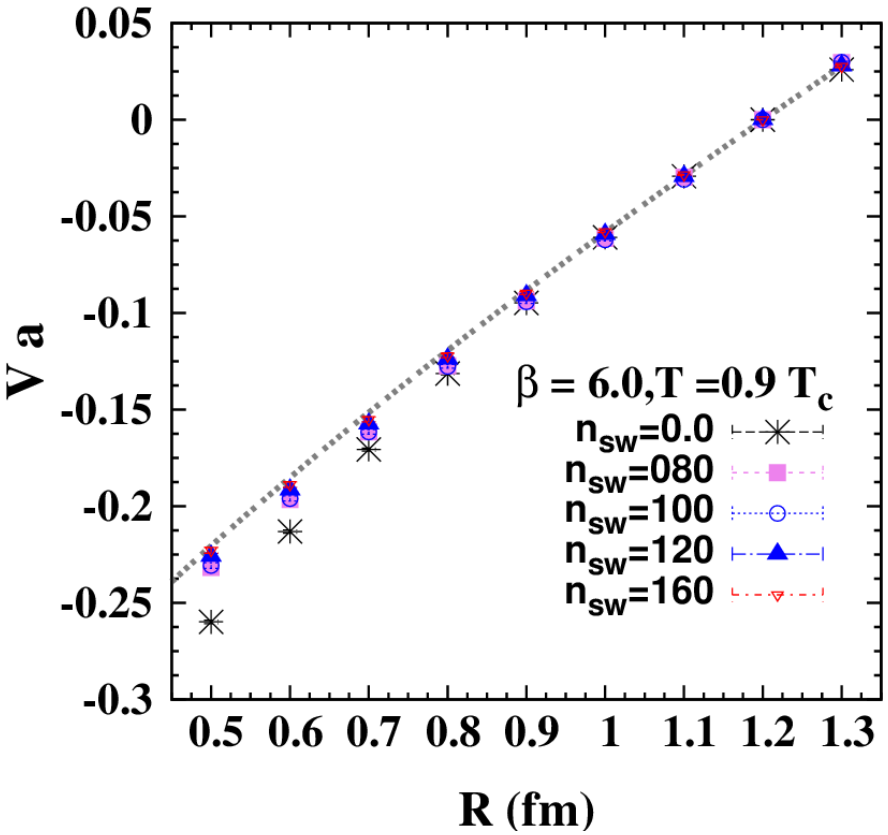

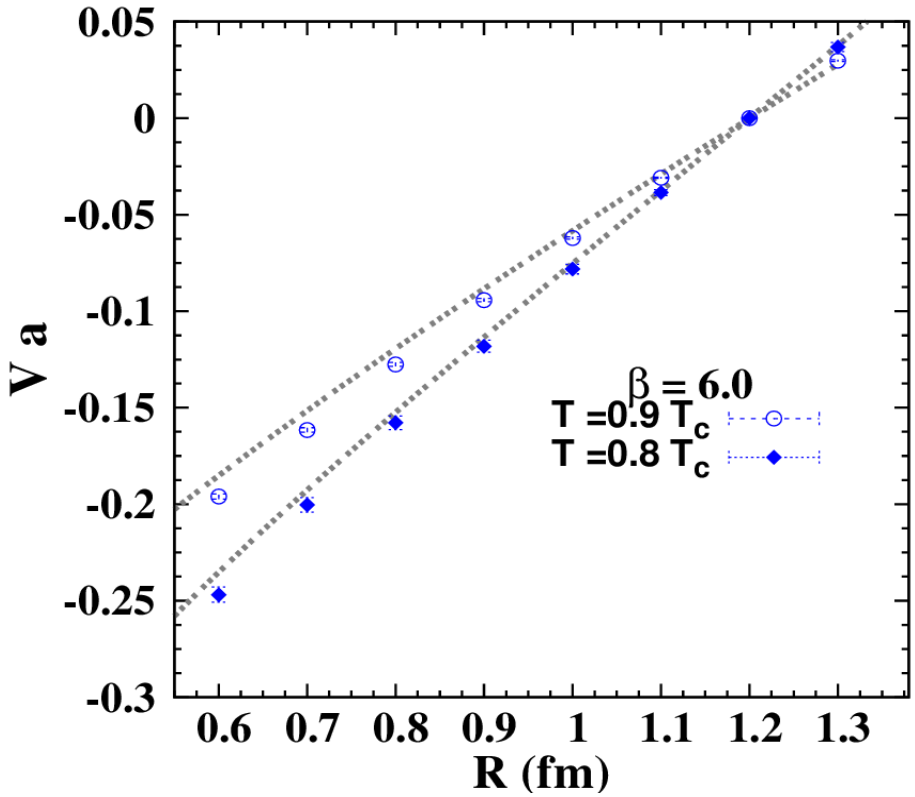

- Based on the observation that Monte Carlo updating of the three-dimensional smeared lattices preserves the key features of the long distance physics.

Table 1. The percentage difference in the quark–antiquark potential relative to the string model predictions[36] calculated as, $|(V_{\rm model} - V_{\rm Lattice})/V_{\rm model}|$, at two temperatures and for the corresponding quark separation.

Temperature/Distance	$R = 0.5$ fm (%)	0.6 fm (%)	0.7 fm (%)	0.8 fm (%)	0.9 fm (%)
$T/T_c = 0.8$	16.8	15.4	13.6	11.1	7.8
$T/T_c = 0.9$	26.1	22.4	18.5	14.2	9.03

Table 1 indicate the decrease in this discrepancy by the decrease of the temperature.

In the intermediate separation region

The effect of 100 sweeps of smearing on the quark–antiquark potential decreases in a similar fashion with the decrease of the temperature.

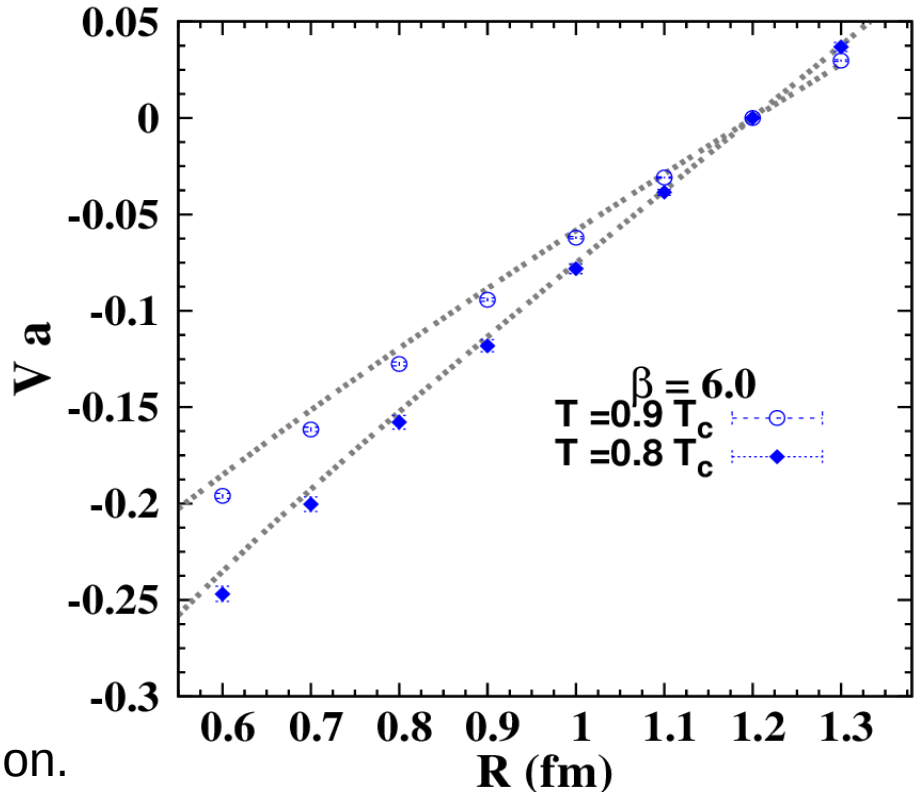

The data eventually approach the string model predictions in the intermediate region.

At zero temperature, the data eventually reaches string model predictions and 3D smearing should have no effect on the potential.

Surface plot of the action density measured at T /Tc = 0.9 in the quark–antiquark plane. The measurements are taken on 100 sweeps of smearing with the lattice divided into two time-slices.

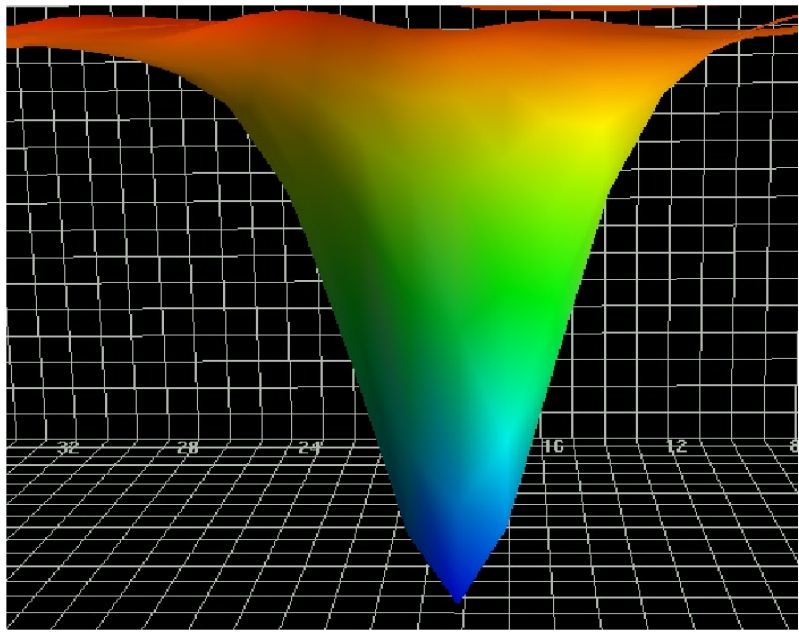

We expect that the inclusion of the 3D smearing into the LW updating cycles would contribute to the efficiency of the LW algorithm for simulations at low temperatures, where the signal is more noisy for large loop sizes and a significant number of updates are required.

At low temperatures, the string predictions would match the lattice data in the intermediate region and hence no significant dependence on the UV physics is expected for this region.

- **Ahmed S. Bakry, Xurong Chen, Pengming Zhang. IJMP E 07/2014; 23(6):1460008**

Lattice results and Y-string model

In the next two section we show an analysis of the lattice data from two points of view.

First , we give a qualitative description of the rendered action density profile and show how the aspects of the distribution are consistent with the stringlike behavior.

Second, we directly compare the width profile of the action density with the string model fluctuations in the following ……

a)filled Delta-shaped

The action density is not of the form of a flux tube that form around the perimeter of the triangle. The distribution maximum is inside the triangle.

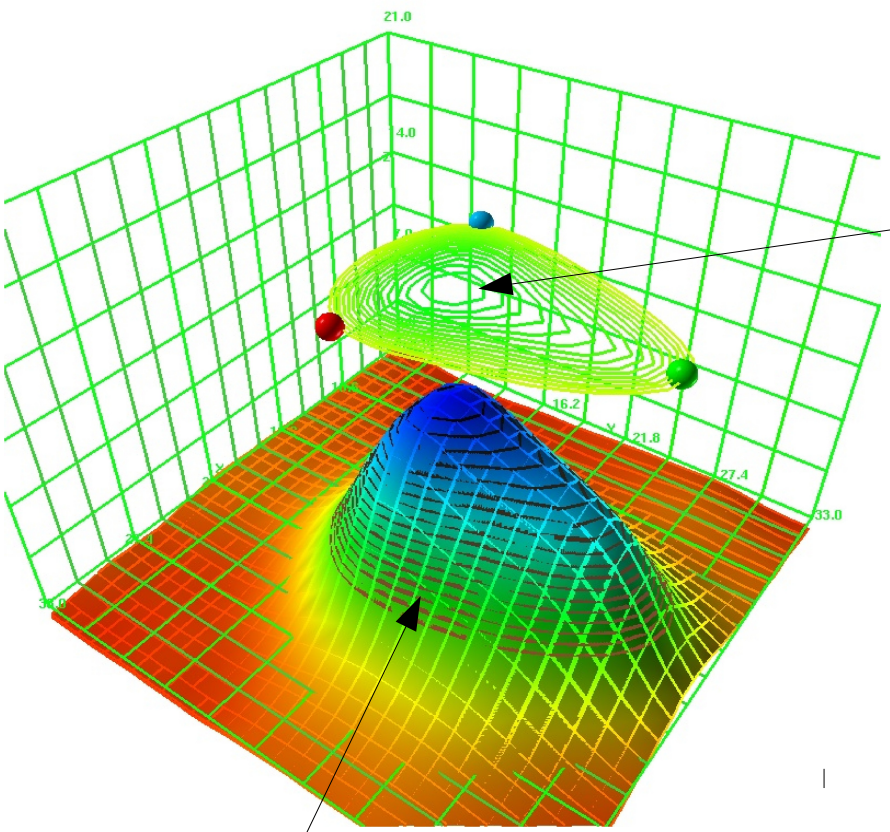

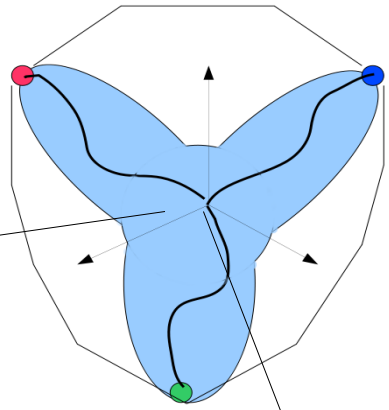

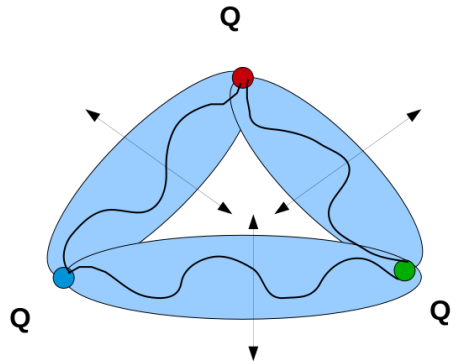

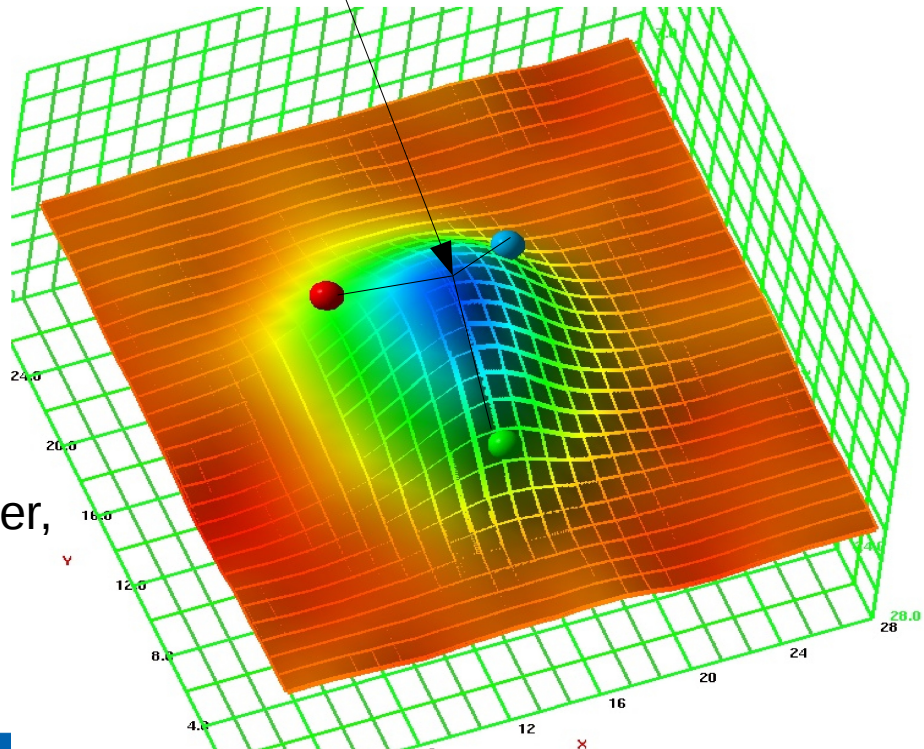

The fast gradient of the scalar field is what causes the action isolines to be denser at the edges, however, the action maximum is inside the triangle.

The best choice of the fitting functions should be based on our experience of the good fit of a single string.

For simplicity, we adopt the approximation where the action density distribution due to a delocalization of a single string can fit to a Gaussian form.

$$G(y;w) = A\exp(-(y)^2/W^2)$$

This is compatible with the degree of accuracy of our lattice data

A. Bakry et al., Phys. Rev. D 82 (2010) 094503,

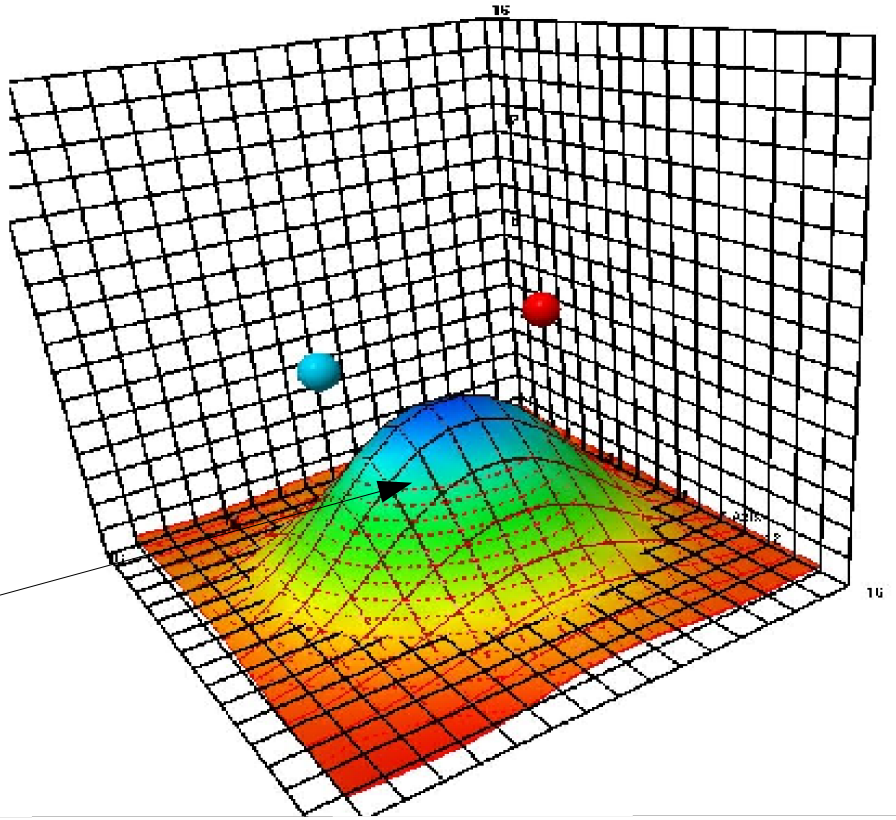

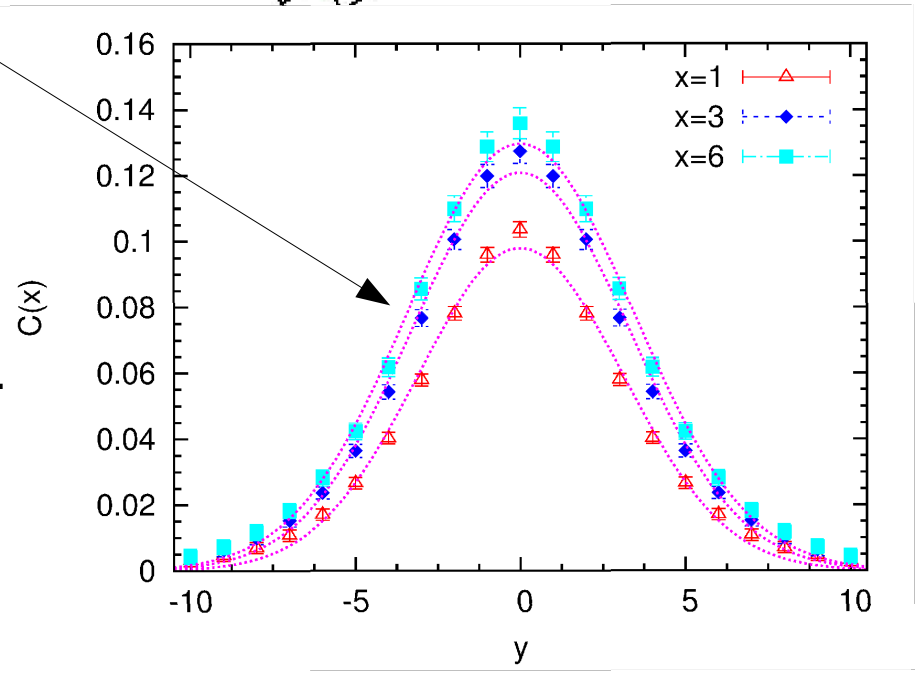

See also
M. Caselle, F. Gliozzi, U. Magnea, and S. Vinti, Nucl. Phys.B460, 397 (1996), hep-lat/9510019

b)The Delta-action is a sum of three Y “Gaussian-Like flux tubes”

To unravel the configuration of the strings in the baryon, we explore the structure of the gluonic distribution with a general ansatz consisting of a two Gaussians

$$G(y; a, w) = A\exp(-(y-u)^2/W^2) + A\exp(-(y+u)^2/W^2).$$

The form assumes a region consisting of a system of two overlapping strings of the same strength A, and mean-square width.

We scan the gluonic domain with the above fit function for all the distances x from the base A connecting the quarks Q1 and Q2 .

The interesting behavior comes from the returned values of the parameter u.

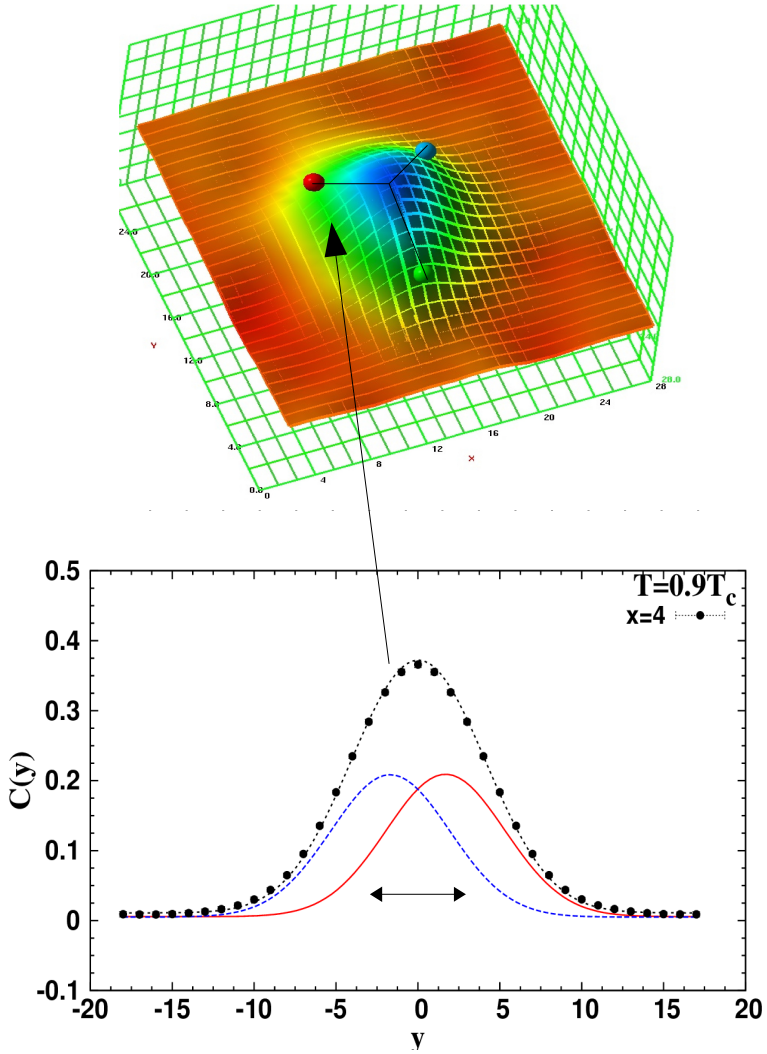

The two-Gaussian profile

The plots shows how the separation between the two Gaussian varies with the movement of third quark and with the length of the triangle base A.

We call the position x, at which u(x)=0, the mean position of the junction.

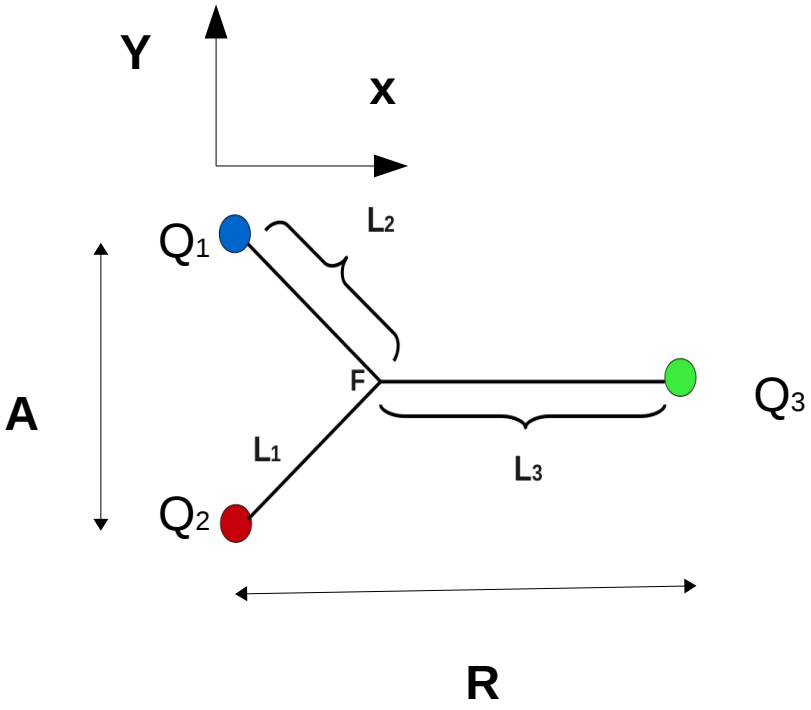

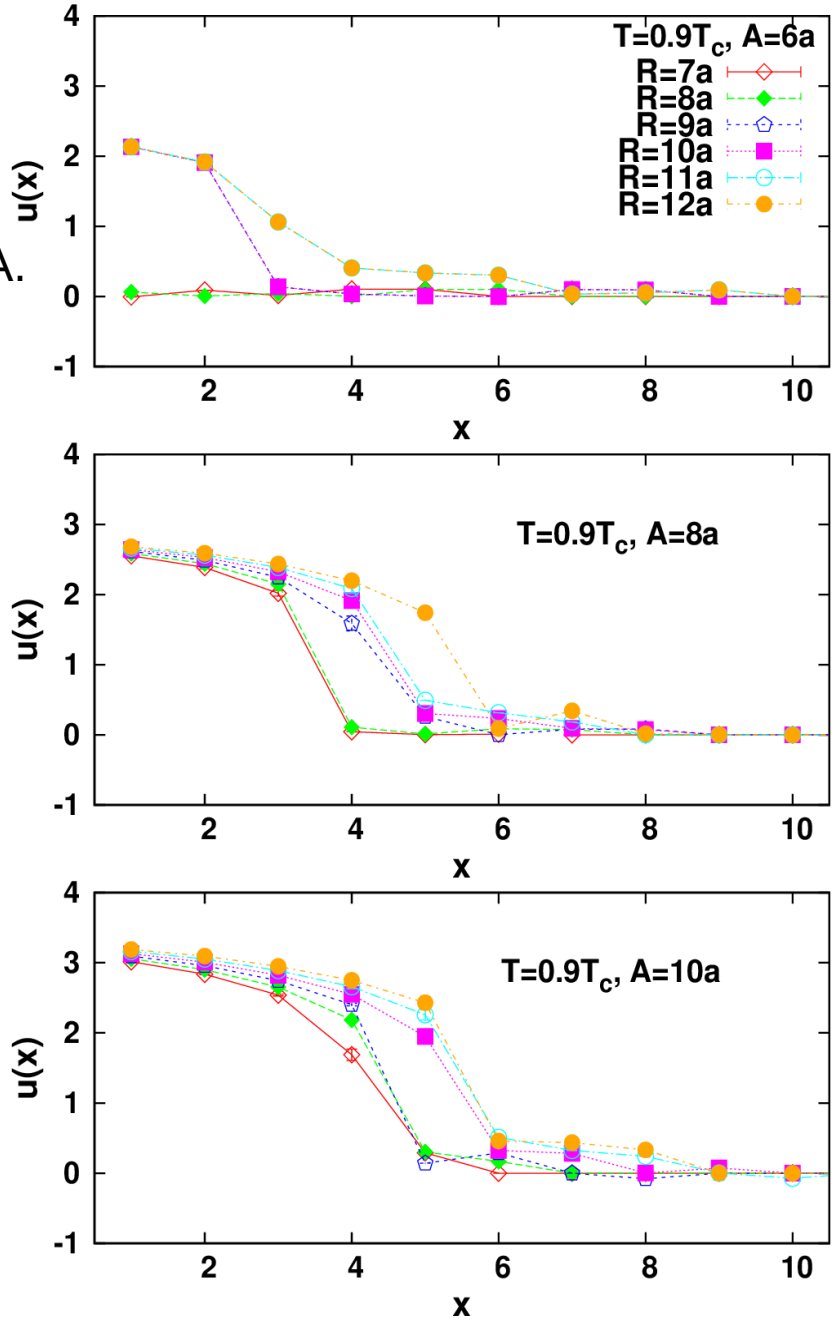

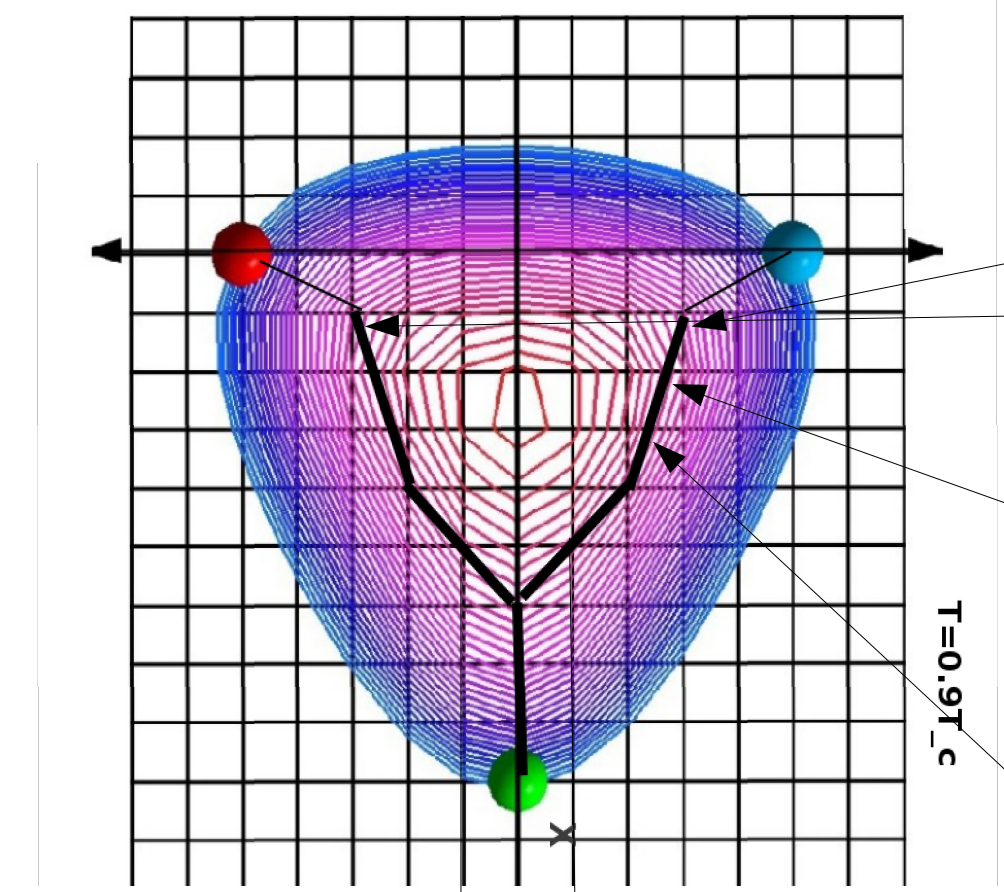
T=0.9T_c
x

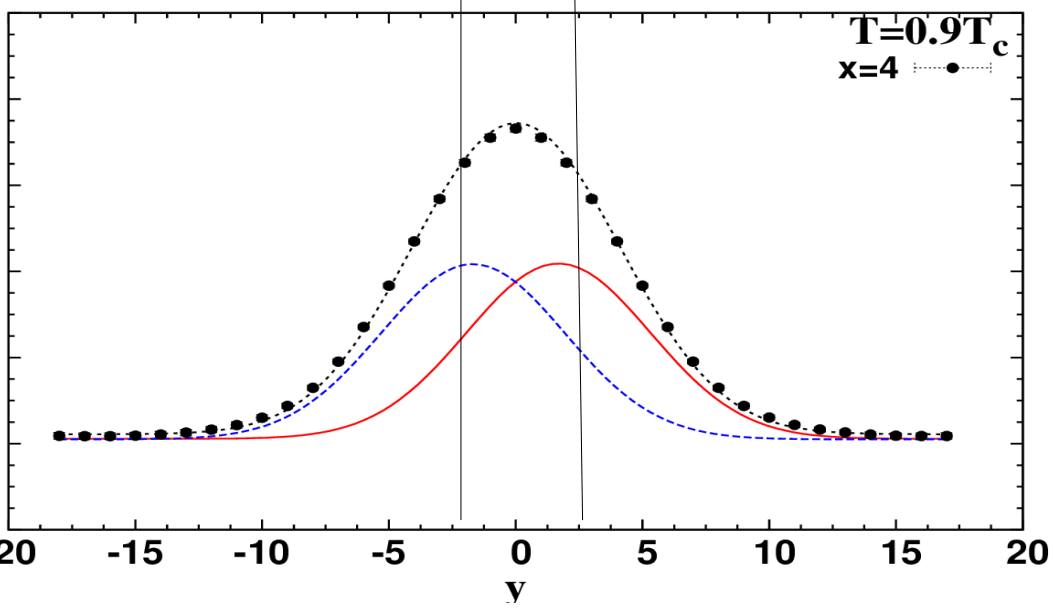
T=0.9T_c
x=4
C(y)
y

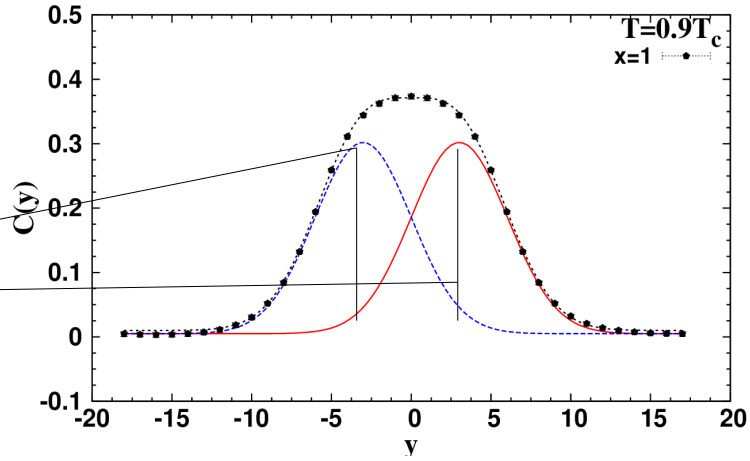
T=0.9T_c
x=1
C(y)
y

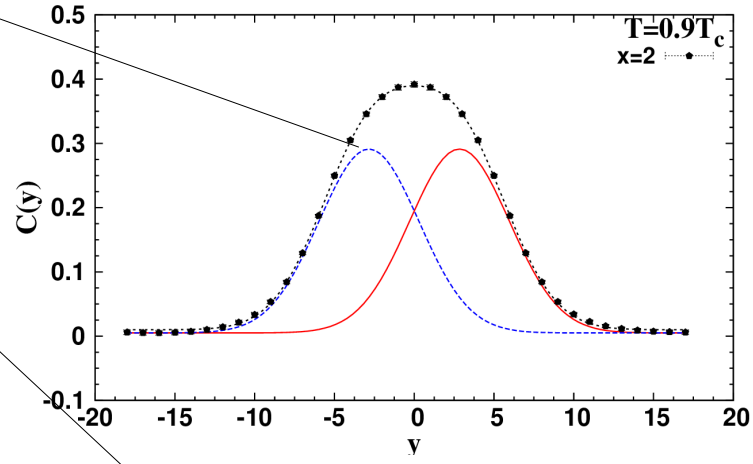
T=0.9T_c
x=2
C(y)
y

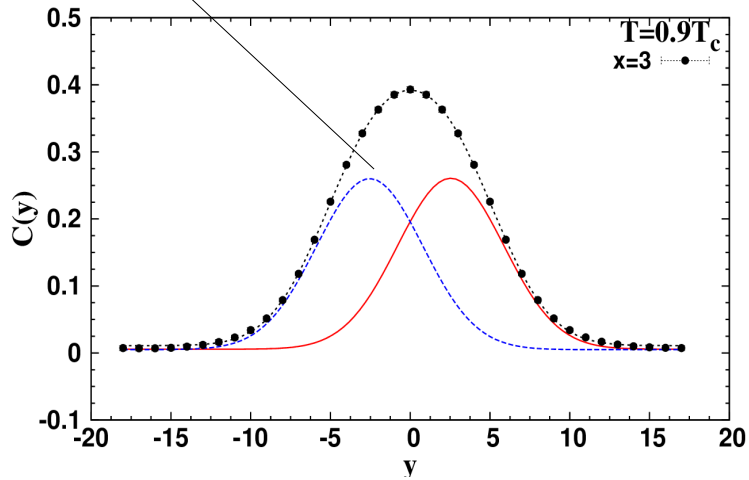
T=0.9T_c
x=3
C(y)
y

Compares the two string profiles at two-temperatures

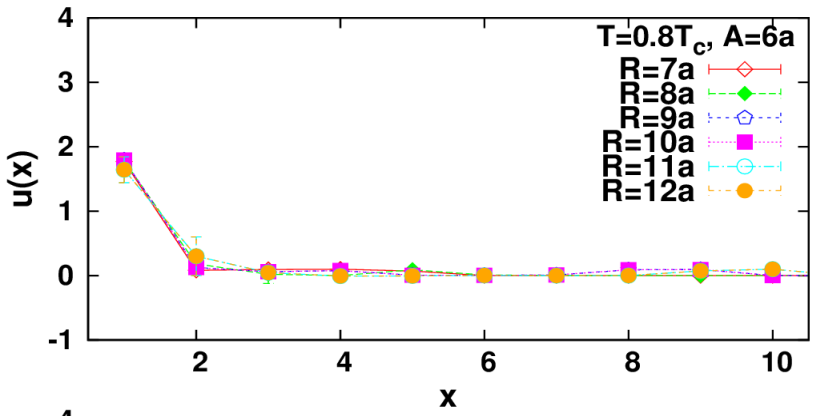

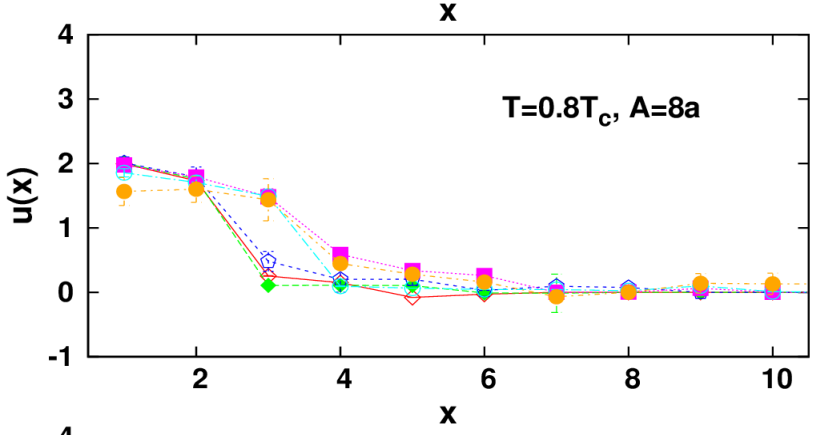

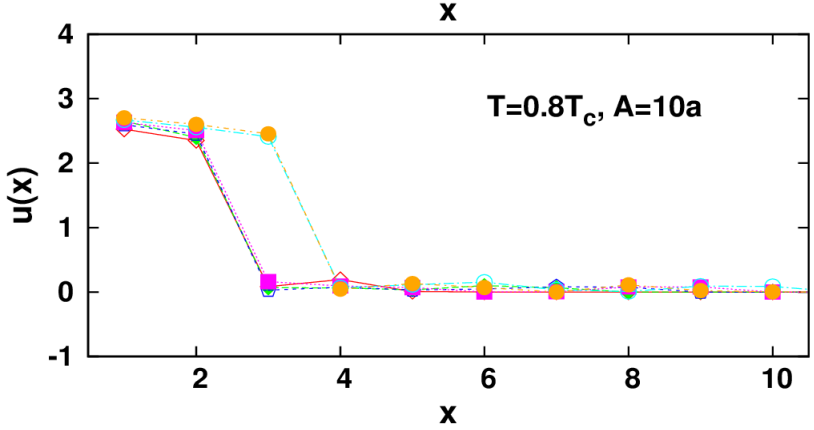

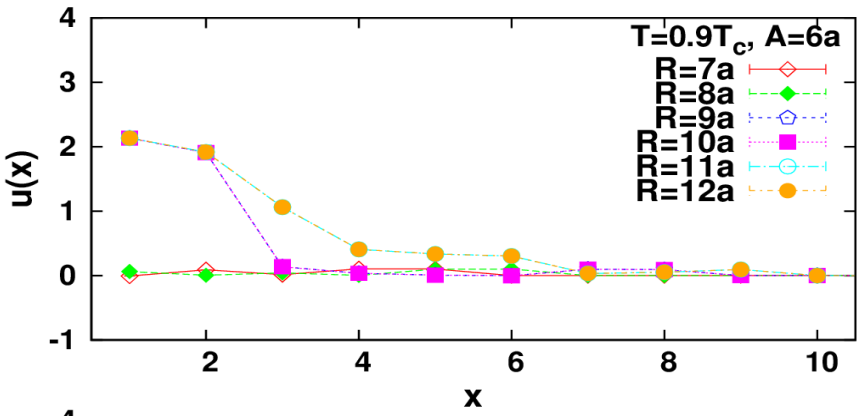

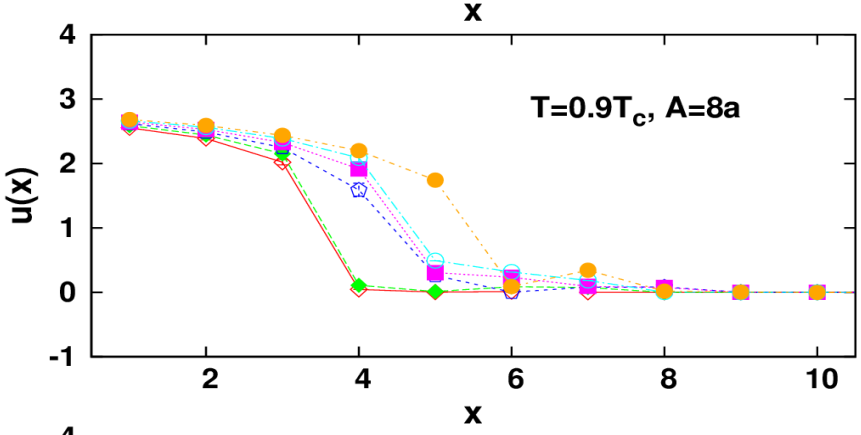

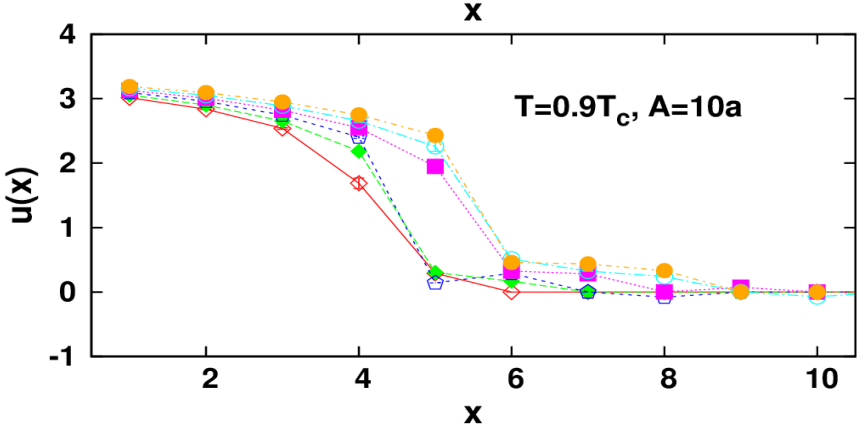

T=0.8T$_c$

T=0.9T$_c$

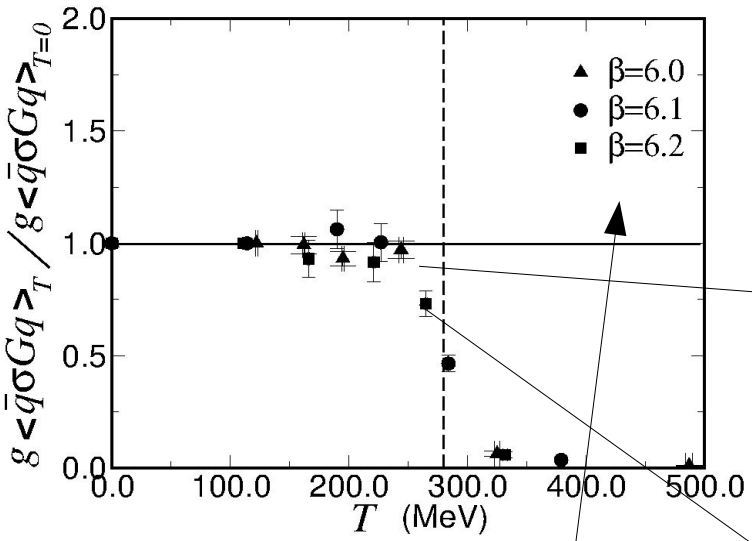

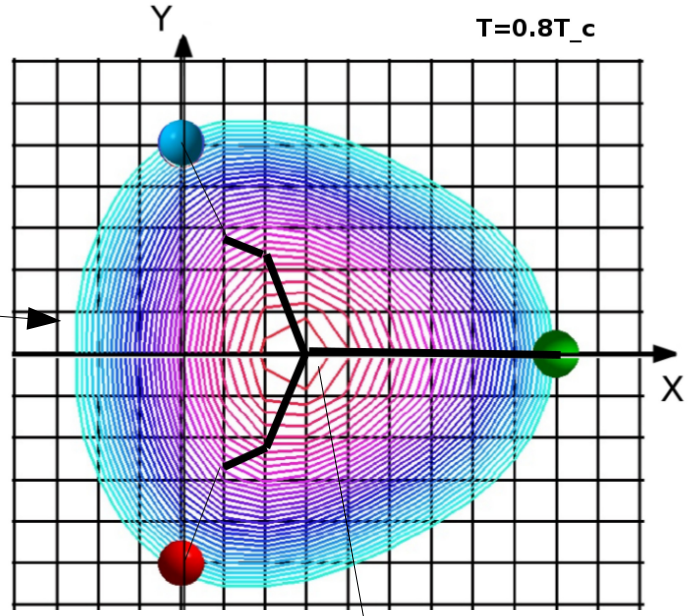

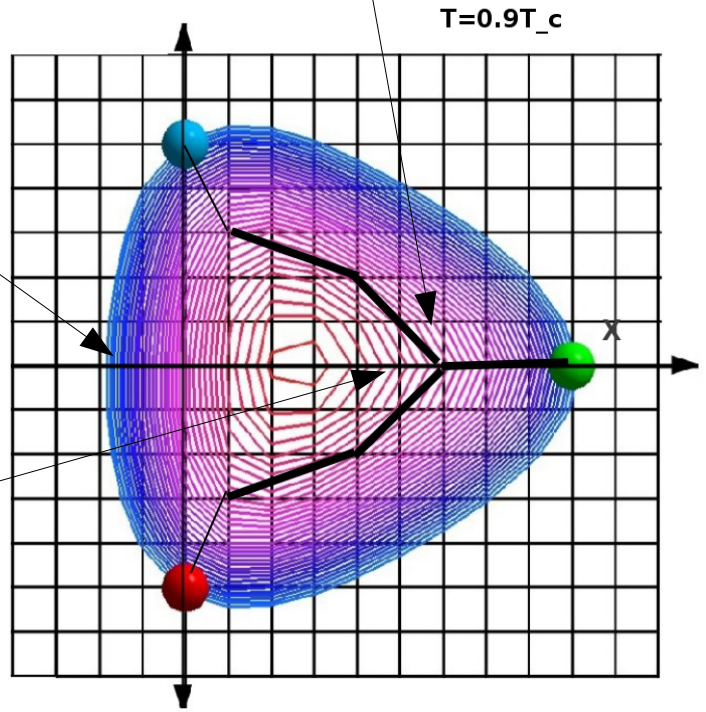

The revealed color map in mesons and baryons at this temperature can be speculated as exhibiting similar behavior to that at low and zero temperatures.

The change in string tension with temperature near the end of QCD plateau is roughly 10%.

The movement of the junction with the increase of the temperature.

- Minimal length for the Y-Profile at the end of QCD plateau, Maximum near deconfinement point.

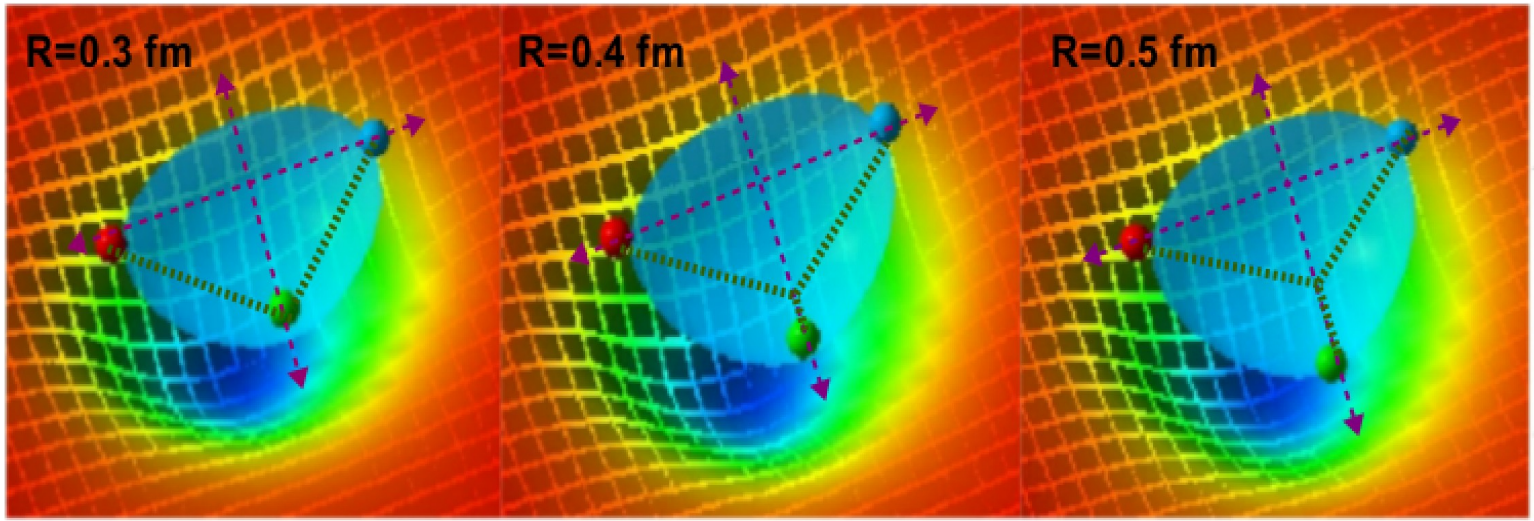

This a schematic plot of the profile of the two Gaussians
Superimposed over the rendered action density.

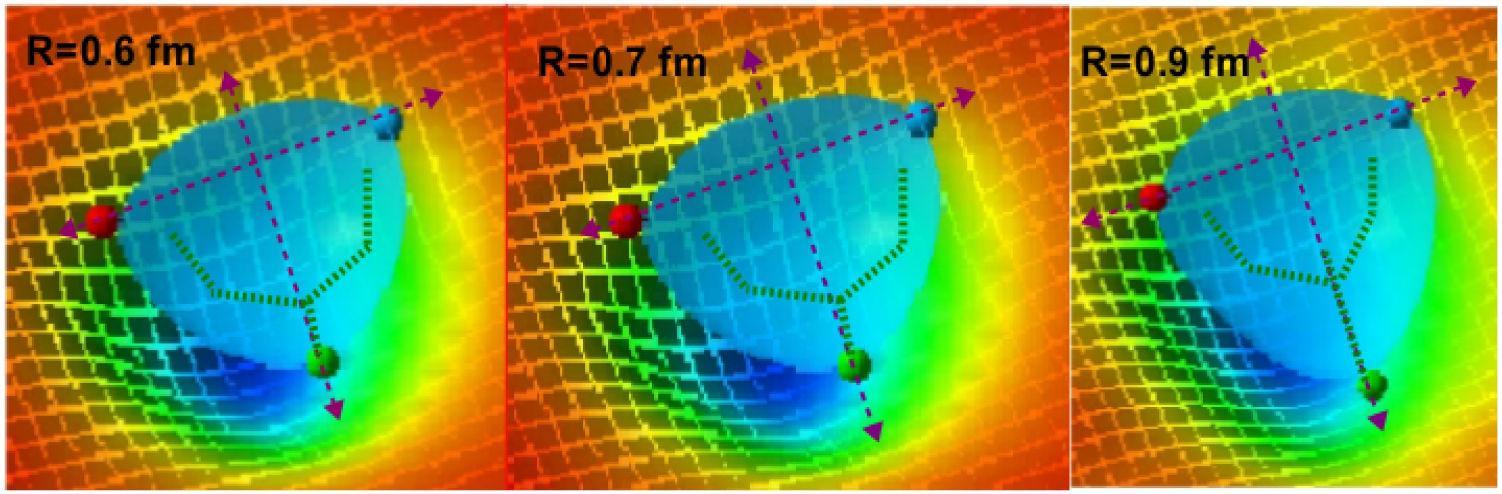

The profile at larger quark separation is clear Y-shaped.

The transverse profile of the action density fits to a double humped function indicating a system of overlapping strings-like flux tubes.

The revealed configurations of these Gaussian flux-tubes show dynamical aspects and reconfigure with respect to the quark configuration and temperature.

The string picture indicates an asymmetry in the mean- square width between the two planes.

M. Pfeuffer, G. S. Bali, and M. Panero, Phys. Rev. D 79, 025022 (2009).

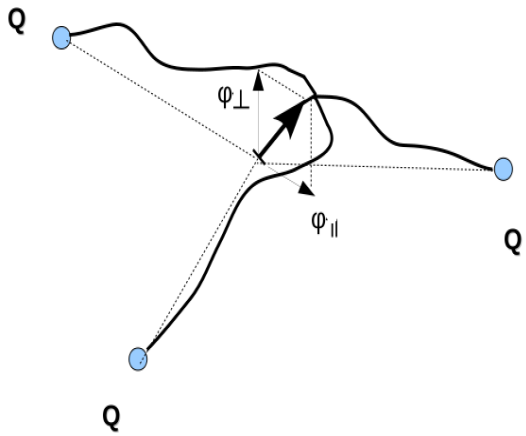

The action density using the Wilson loop does not appear to produce an asymmetric gluonic pattern.

F. Bissey et al., Phys. Rev. D 76, 114512 (2007), hep-lat/0606016.

Y-Wilson loop

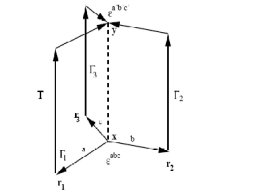

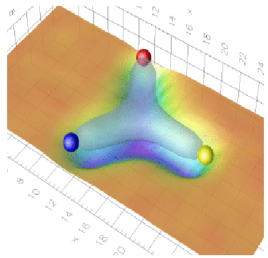

The radius of the tube is calculated with cylindrical co-ordinates assuming a cylindrical symmetry of the tube.

Aspect Ratio

$$\alpha(x) \equiv \frac{W_y^2(x)}{W_z^2(x)}.$$

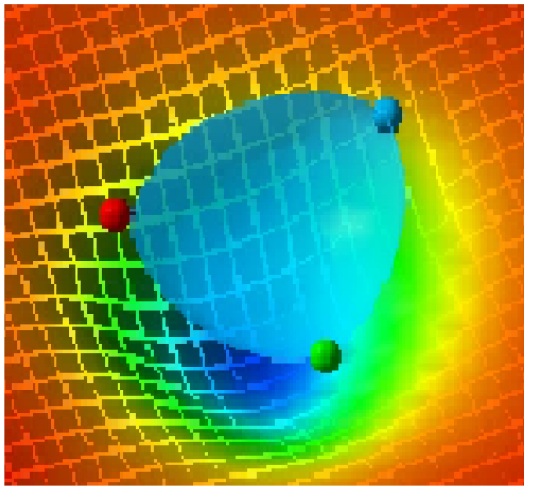

The aspect ratio at the temperature T /Tc = 0.8 for the indicated quark configurations.

Generally, the aspect ratio is greater than 1 for planes x ∈ [0,8] indicating that in-plane fluctuations are greater than the perpendicular fluctuations.

This results are consistent with a greater restoring forces in the quark planes for the Y-string-like gluonic distribution.

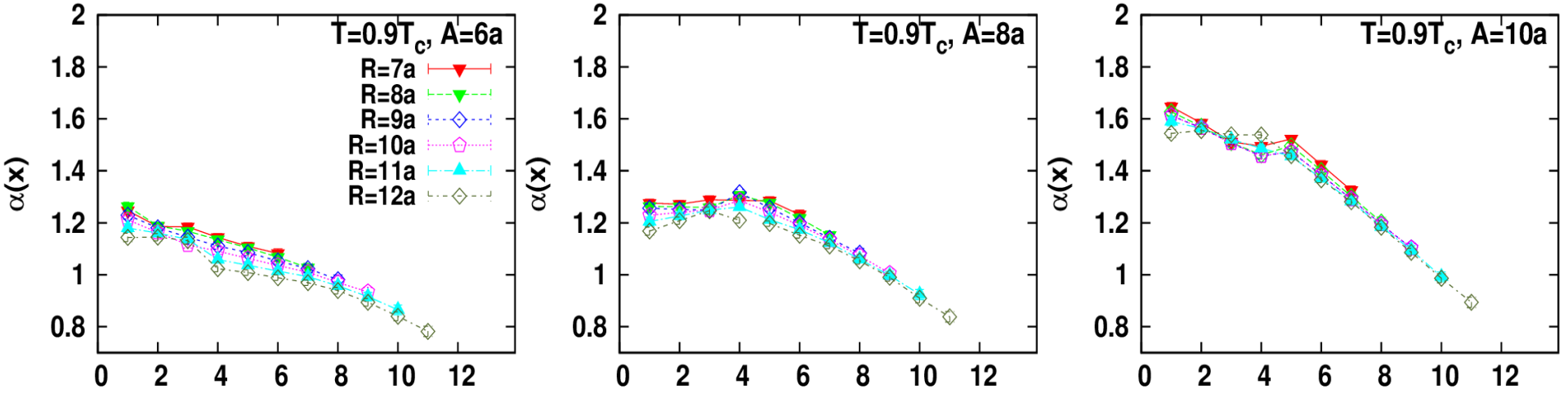

Summary of qualitative properties

- Filled Delta Shape Flux profile.
- The Delta shape is a sum up of three Y-shaped Gaussian string profile.
- Minimal length for the Y-Profile at the end of QCD plateau, Maximum near deconfinement point.
- The aspect ratio indicates a larger restoring force in the quark plane.

Broadening of the flux tube

The broadening of the flux tube with the increase of the source separation is compared to the corresponding string model predictions.

This can provide a first indication of the compatibility of the baryonic string model with the measured LGT junction profile, the position of the junction and its proposed insight.

The Y-string's configuration has to be fixed before proceeding to fits with the lattice data.

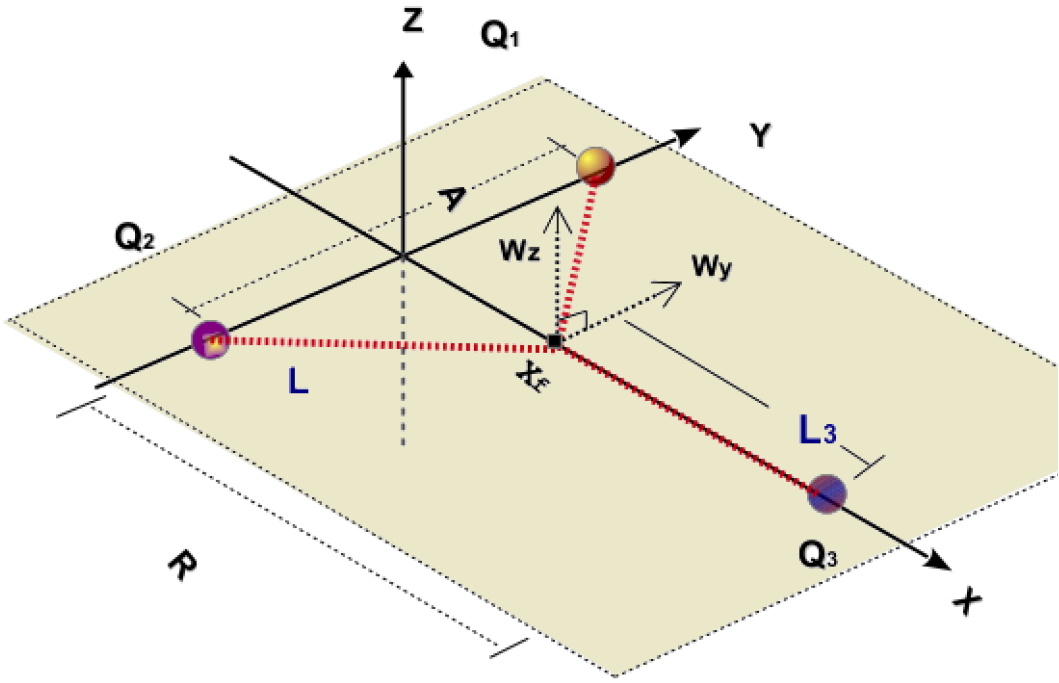

The proposed string configuration with respect to the quark positions.

Returned fits of the gluon flux to the string width profile

a) In-plane fluctuations

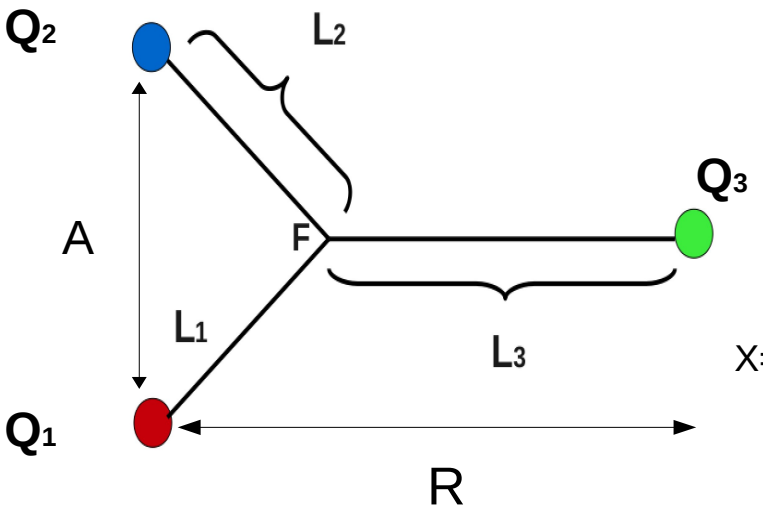

X=1, A=0.6 fm, X_f =1.7

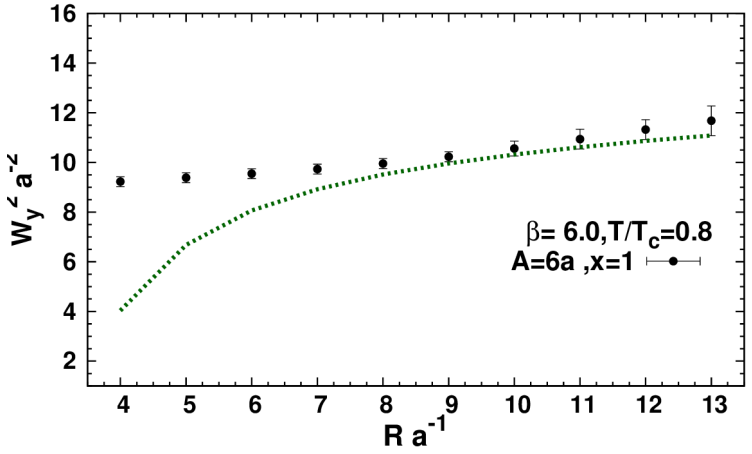

X=2, A=0.8 fm, X_f =2.3

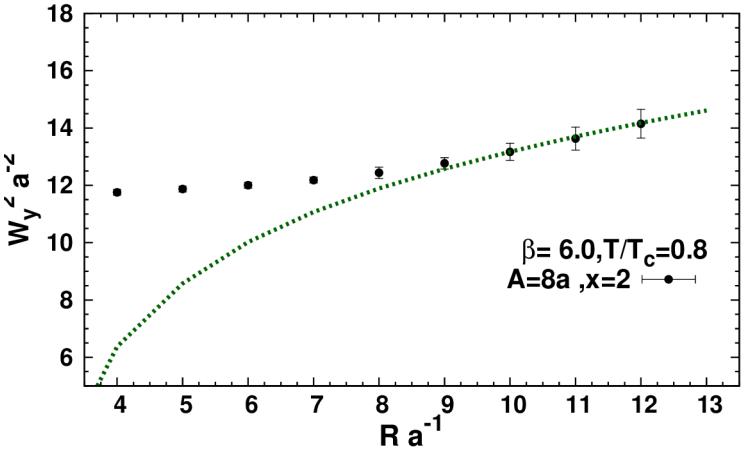

Fits of the junction's profile from string picture to the lattice data.

The broadening of the width versus the third quark separation R.

X=2, A=1.0 fm, X_f =2.9

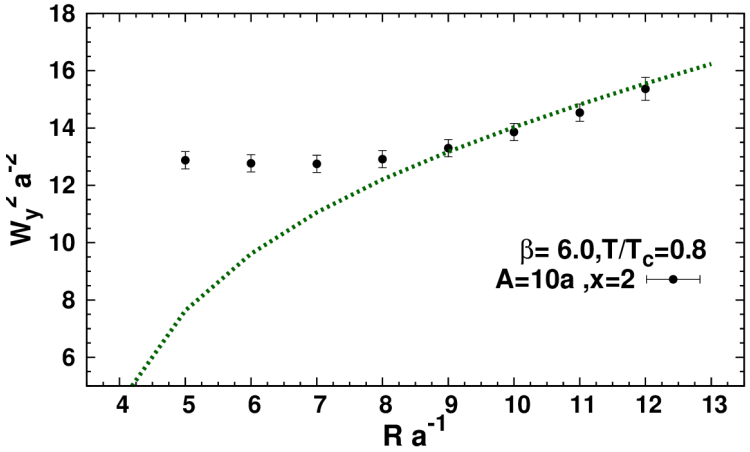

Returned fits of the gluon flux to string width profile

a) In-plane fluctuations

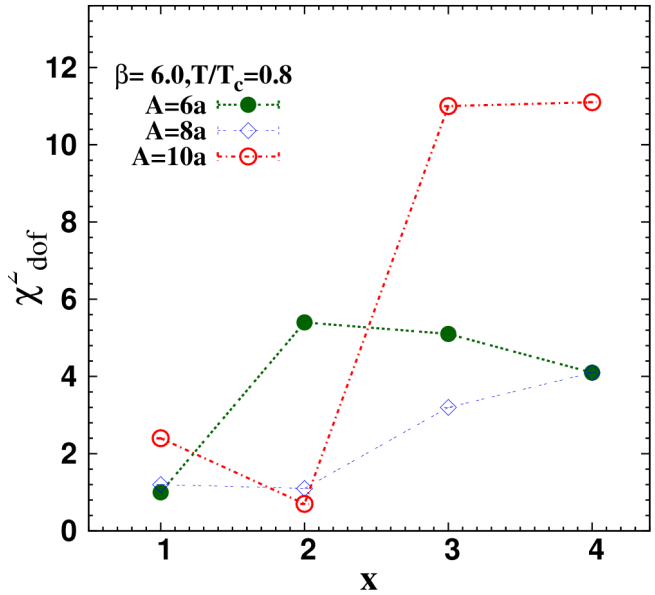

X=1, X_f =1.7

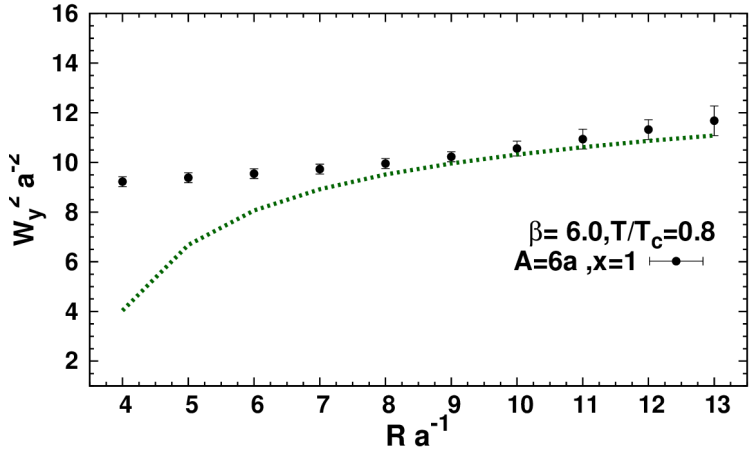

The best returned fits are near the position of Fermat point for the temperature T/T_c=0.8

X=1, X_f =2.3

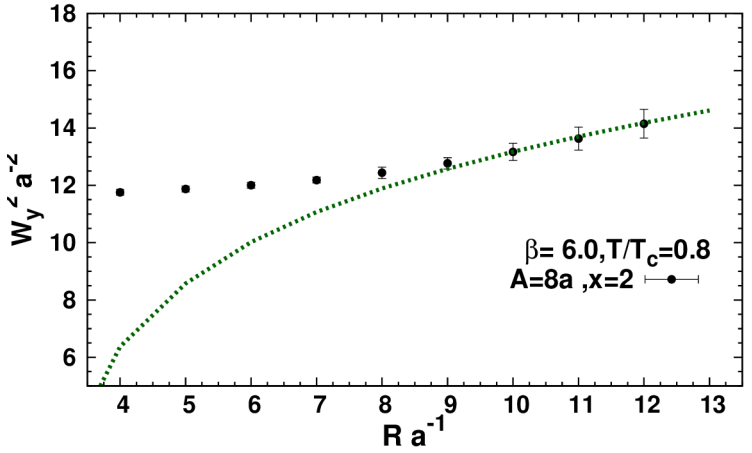

The existence of particular planes at which best matches are found suggests that some planes receives a larger contribution of the junction's fluctuations.

X=1, X_f =2.9

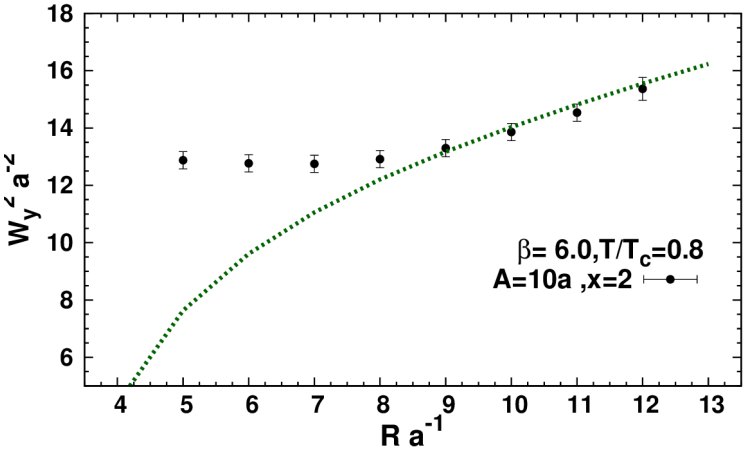

The string profile at higher temperature just before the deconfinement

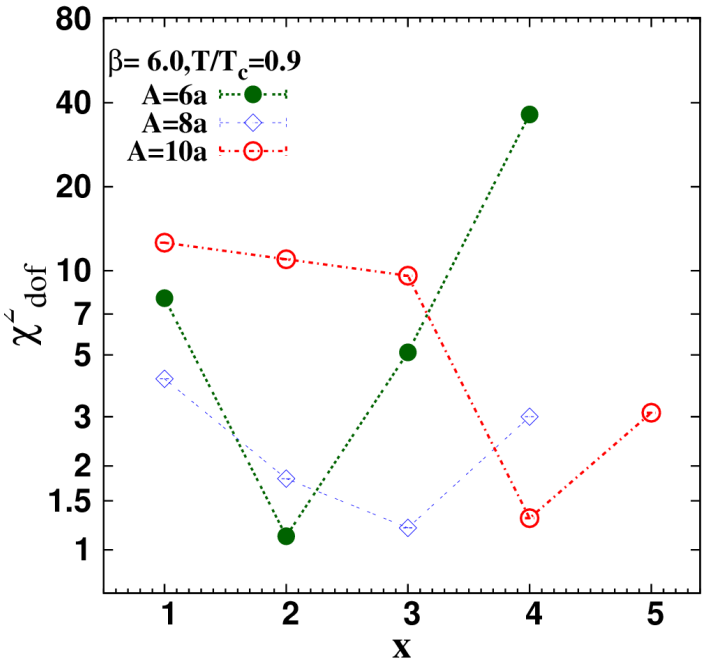

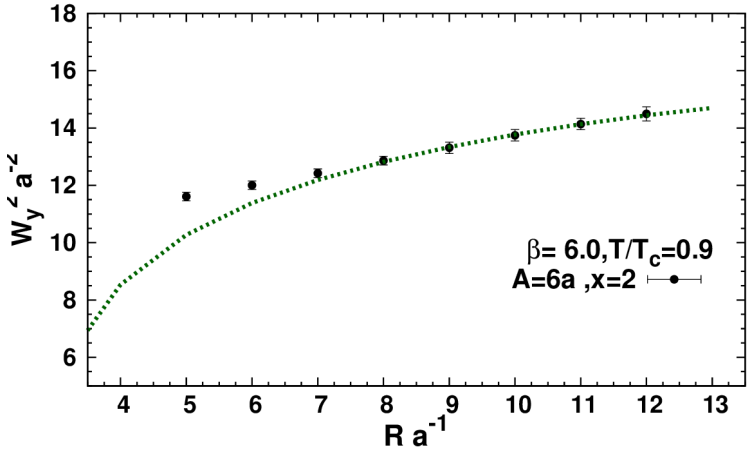

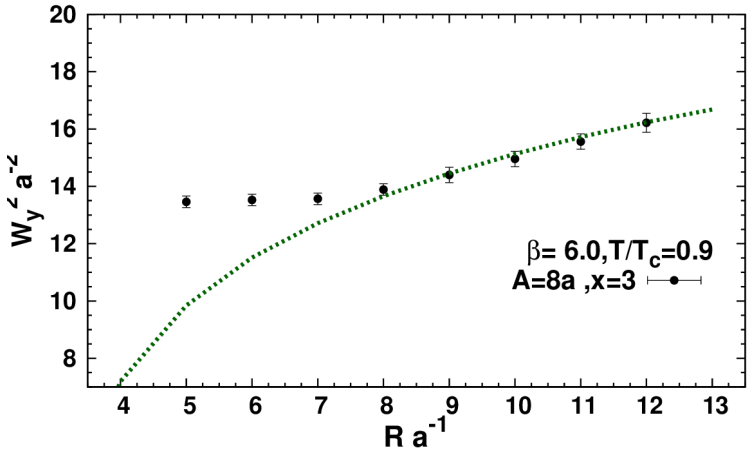

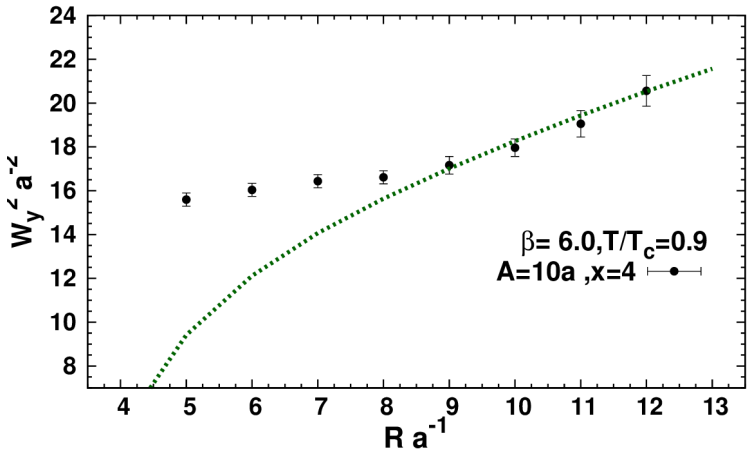

At higher temperature T/T_c=0.9, the best returned fits are not in accord to the closest plane to the string's junction.

At both temperature, the Y-string picture at finite temperature poorly describes the lattice data at short distances.

We observe that the planes of best fits manifest in accord with the profile of the two Gaussian shown rather than junction's classical position at the Fermat point.

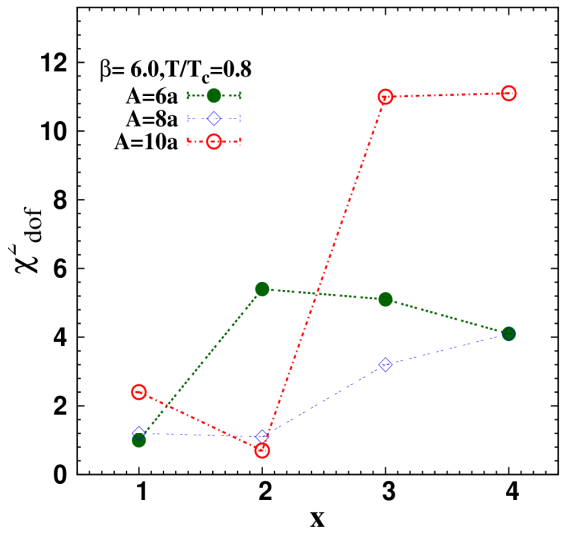

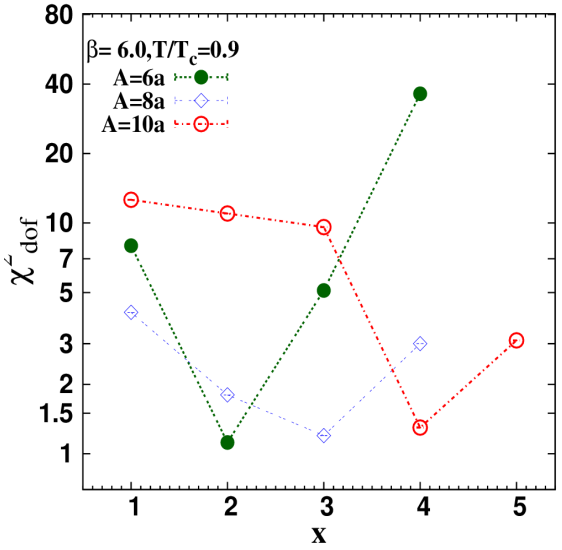

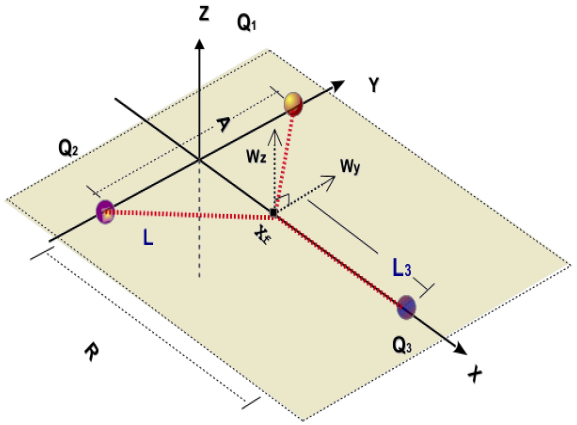

A=1.0 fm

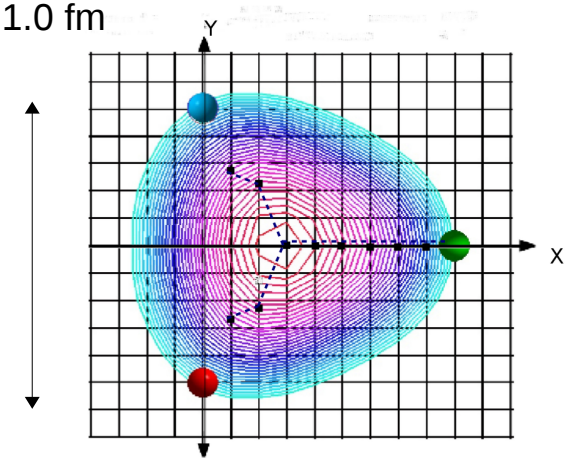

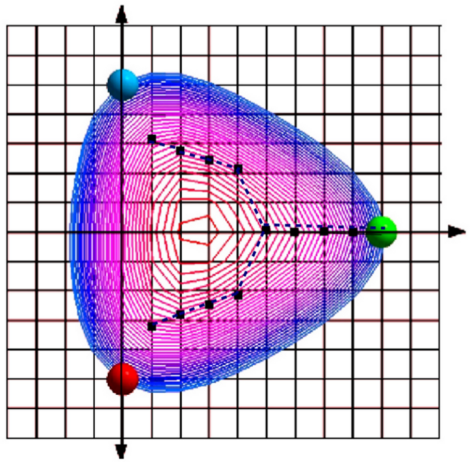

The greatest contribution of the junction appears to be in one lattice spacing immediately before the plane at which $u(x_0) = 0$.

b)Perpendicular Fluctuation

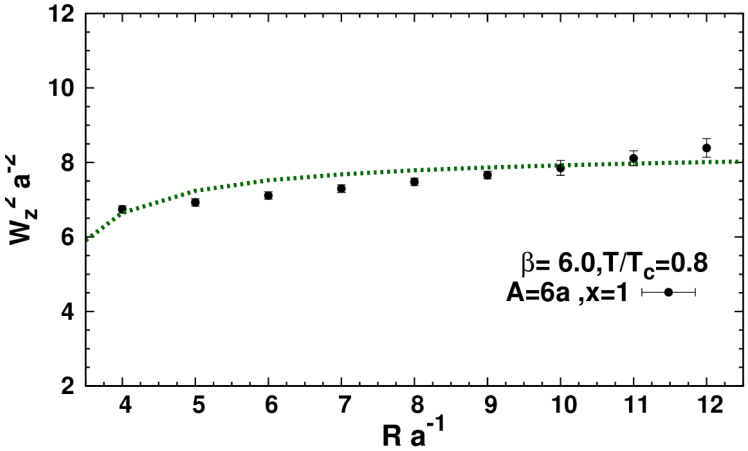

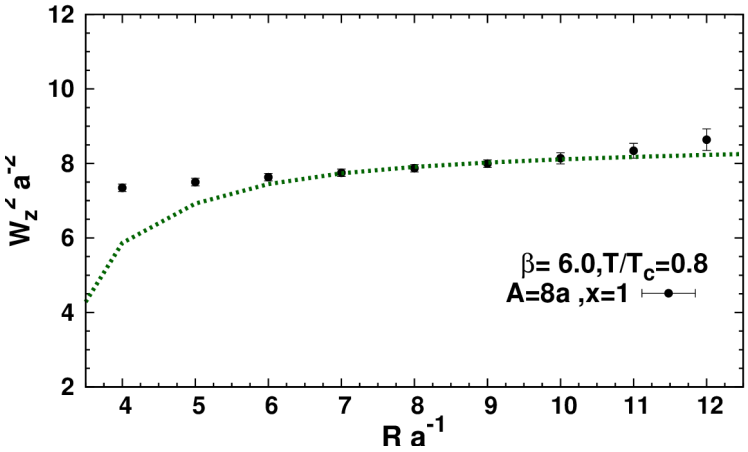

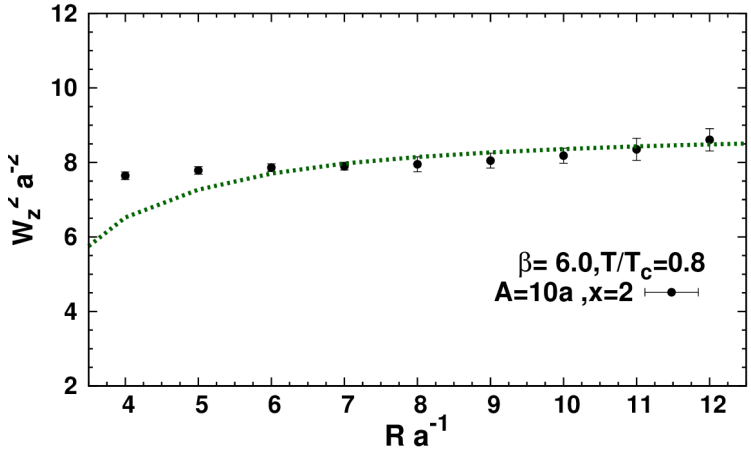

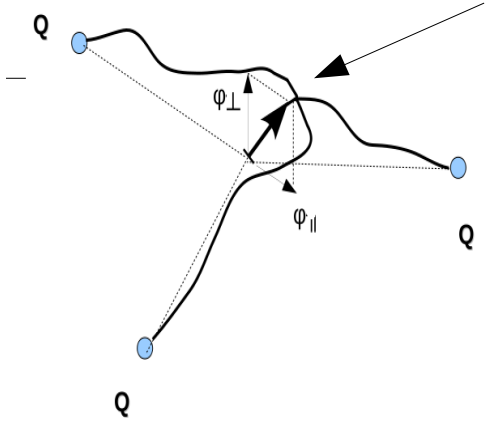

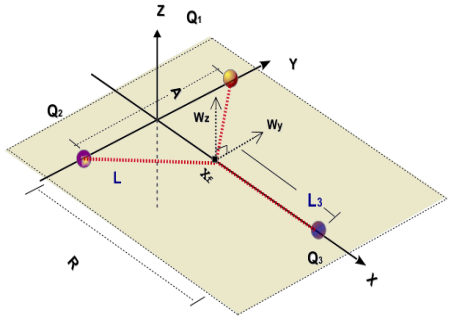

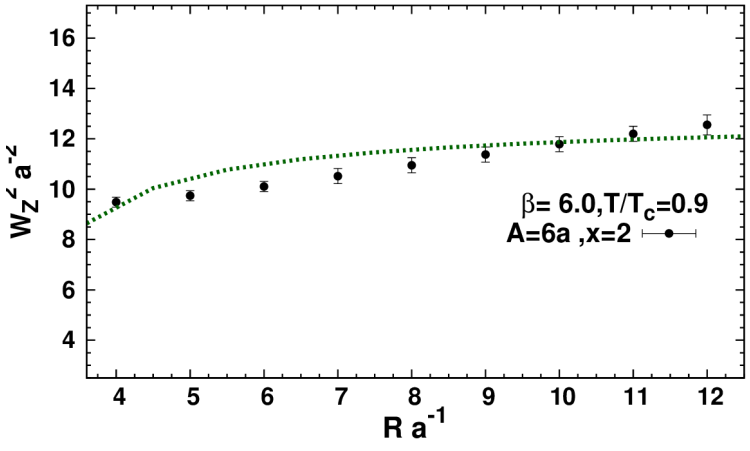

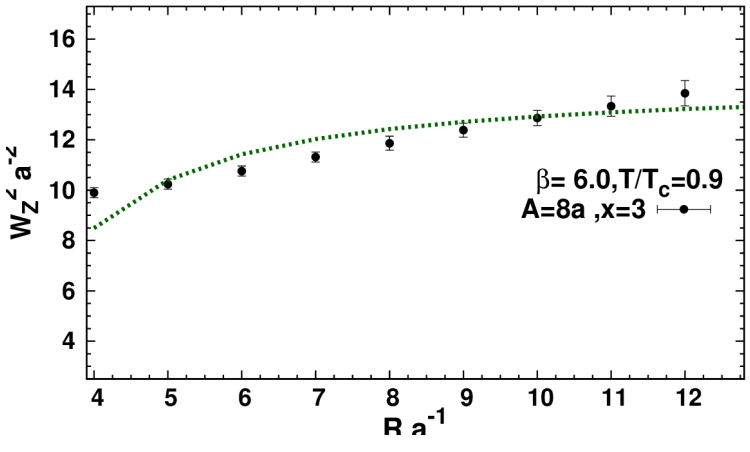

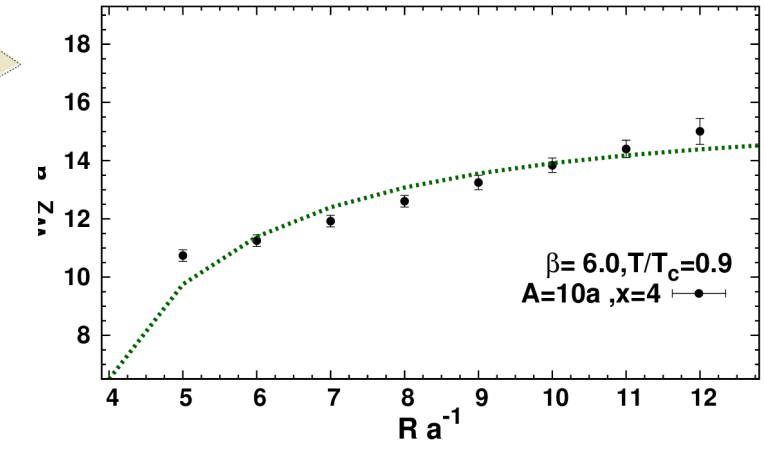

For perpendicular fluctuations, we still obtain the best fits at the same planes obtained for the in-plane action-density width.

From the above discussion, we conclude that the Y-string picture with a minimal length of the string entails a mean-square width of its quantum fluctuations which is consistent with the lattice-gauge data at large color-source separation.

“Y-string-like behavior in a static hadron at finite T”, Ahmed. Bakry, Xurong Chen, Pengming Zhang. Hep-lat/1412.3568. To be submitted to PRD.

Summary

- Qualitative analysis of the density plots suggests string profile

  (Filled-Delta, three --Y-shaped-- Gaussian flux tubes, Aspect ratio < 1)

- The Y-baryonic string model has been discussed at finite temperature for the width profile of the junction assuming it's classical position at Fermat point.

- The lattice data for the mean-square width of the gluonic action density has been compared with the string width.

- The best fits for the string model are returned for large quark source separation.

- We report a formation of the Y-shaped confining strings in a static baryon at finite T in the action density of Pure SU(3) YM theory for the first time.

- The revealed form of the flux in the baryon presents a potential candidate for the exact geometry of the flux-tubes at zero temperature.

- Noise reduction by including UV filtering step into LW Updating cycle

  in Multi-level algorithm.

  May extent the above analysis in unambiguous way to zero temperature.....

Thank you!